JBC RESEARCH ARTICLE

Fructose-1-kinase has pleiotropic roles in *Escherichia coli*

Received for publication, January 23, 2024, and in revised form, April 26, 2024 Published, Papers in Press, May 8, 2024,
https://doi.org/10.1016/j.jbc.2024.107352

Chamitha Weeramange[1,‡], Cindy Menjivar[2,‡], Pierce T. O'Neil[1,‡], Samir El Qaidi[3], Kelly S. Harrison[4], Sarah Meinhardt[1], Cole L. Bird[1], Shwetha Sreenivasan[1], Philip R. Hardwidge[3], Aron W. Fenton[1], P. Scott Hefty[3], Jeffrey L. Bose[2], and Liskin Swint-Kruse[1,*]

From [1]The Department of Biochemistry and Molecular Biology, The University of Kansas Medical Center, Kansas City, Kansas, USA; [2]The Department of Microbiology, Molecular Genetics and Immunology, The University of Kansas Medical Center, Kansas City, Kansas, USA; [3]College of Veterinary Medicine, Kansas State University, Manhattan, Kansas, USA; [4]The Department of Molecular Biosciences, The University of Kansas – Lawrence, Lawrence, Kansas, USA

Reviewed by members of the JBC Editorial Board. Edited by Chris Whitfield

In *Escherichia coli*, the master transcription regulator catabolite repressor activator (Cra) regulates >100 genes in central metabolism. Cra binding to DNA is allosterically regulated by binding to fructose-1-phosphate (F-1-P), but the only documented source of F-1-P is from the concurrent import and phosphorylation of exogenous fructose. Thus, many have proposed that fructose-1,6-bisphosphate (F-1,6-BP) is also a physiological regulatory ligand. However, the role of F-1,6-BP has been widely debated. Here, we report that the *E. coli* enzyme fructose-1-kinase (FruK) can carry out its "reverse" reaction under physiological substrate concentrations to generate F-1-P from F-1,6-BP. We further show that FruK directly binds Cra with nanomolar affinity and forms higher order, heterocomplexes. Growth assays with a Δ*fruK* strain and *fruK* complementation show that FruK has a broader role in metabolism than fructose catabolism. Since *fruK* itself is repressed by Cra, these newly-reported events add layers to the dynamic regulation of *E. coli*'s central metabolism that occur in response to changing nutrients. These findings might have wide-spread relevance to other γ-proteobacteria, which conserve both Cra and FruK.

The ability of a microorganism to respond to external stimuli, such as changes in available carbon sources, requires the ability to switch between alternative metabolic programs. Many switches are accomplished by the activity of transcription factors that control the expression of different groups of metabolic genes. In γ-proteobacteria, one of the most important transcription factors is the catabolite repressor activator protein (Cra; UniProt P0ACP1). In *Escherichia coli*, Cra differentially regulates genes important to glycolysis, TCA cycle, gluconeogenesis, and the Entner-Doudoroff pathway (1–6) so that glucose metabolism is repressed when gluconeogenesis is activated. A key step of this regulatory process occurs when Cra binds fructose metabolite(s) that, in turn, allosterically diminish Cra's binding to DNA (7).

An unambiguous finding is that fructose-1-phosphate (F-1-P) can act as a strong Cra allosteric inhibitor at micromolar concentrations (7). However, the biological source(s) of F-1-P and whether it is the only fructose metabolite that allosterically regulates Cra has engendered some controversy. To date, the formation of F-1-P has only been documented as arising from the coincident import and phosphorylation of exogenous fructose by FruBA (Fig. 1; (8–12)). However, it is something of a paradox that F-1-P from exogenous fructose would serve as the only molecular switch for this central metabolic network. Indeed, results from a variety of biological studies (*e.g.*, (13–17)), are consistent with the proposal that millimolar concentrations of fructose-1,6-bisphosphate (F-1,6-BP) also regulate Cra's activity (7). Since F-1,6-BP is a metabolic intermediate for many sugars, this would allow Cra to be regulated in a wide variety of nutrient conditions.

However, it is unlikely that F-1,6-BP directly binds to Cra: In an early study showing a weak effect of 5 mM F-1,6-BP on Cra's DNA binding, the authors acknowledged that the effect could be due to F-1-P contamination (7). Study of *Pseudomonas putida* Cra supported the contamination hypothesis (18, 19). Most convincingly, a 2018 study of *E. coli* Cra that controlled for F-1-P contamination showed no direct F-1,6-BP binding or induction from the $fruB_{distal}$ DNA operator–binding site (20).

Efforts to experimentally assess and model the Cra regulon have not helped to clarify the role of F-1,6-BP or the source of F-1-P: In one study, Cra was proposed to act as a flux sensor that uses intracellular F-1,6-BP to integrate information from a variety of nutrients (16). However, most of the *in vivo* F-1,6-BP concentrations measured under the study conditions were less than 1 mM, nearly an order of magnitude lower than that needed for this metabolite to weakly regulate Cra (7) (if F-1,6-BP can even regulate Cra (20)). A second study to model *E. coli* metabolic flux used F-1-P as the only Cra modulator, but the model predictions could not be reconciled with experimental evidence (21). A third study found that F-1,6-BP, F-1-P, and cyclic AMP were

‡ These authors contributed equally to this work.
* For correspondence: Liskin Swint-Kruse, lswint-kruse@kumc.edu.
Present address for: Chamitha Weeramange, Xencor Inc, 111 W Lemon Ave, Monrovia, CA 91016; Kelly S. Harrison, Department of Veterinary Pathobiology, Oklahoma State University, 166 McElroy Hall, Stillwater, OK 74078; Philip R. Hardwidge, Boehringer Ingelheim, 2412 S Loop Dr, Ames, IA 50010; Samir El Qaidi, Department of Veterinary Pathobiology, University of Missouri, Columbia, MO 65211.

© 2024 THE AUTHORS. Published by Elsevier Inc on behalf of American Society for Biochemistry and Molecular Biology. This is an open access article under the CC BY license (http://creativecommons.org/licenses/by/4.0/).

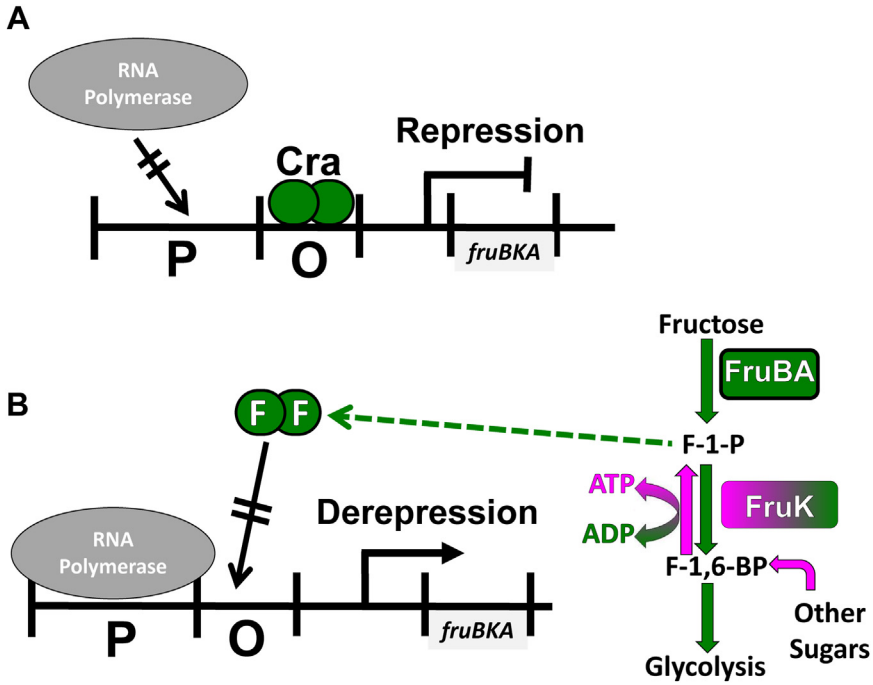

Figure 1. Previously-known activities of Cra and FruK. Protein activities known at the beginning of this work are shown with *green* and known transcriptional responses are shown in *black*. *A*, in the absence of regulatory ligands, Cra binds to operator DNA (O) to regulate the transcription of downstream genes; the example here shows repression of *fruBKA* (7), with "P" indicating the promoter for RNA polymerase (*gray oval*). *B*, the presence of exogenous fructose (*far right*) leads to its concurrent import and phosphorylation by FruBA to create the metabolite F-1-P. In additional to its further metabolism through glycolysis, F-1-P binds to Cra, triggering an allosteric change that diminishes Cra's DNA-binding affinity; the example here shows depression and concomitant transcription of *fruBKA*. In biological assays, metabolism of other sugars *via* F-1,6-BP also appears to regulate Cra's DNA-binding activity (13–17); however, F-1,6-BP does not appear to directly bind Cra (20), raising the question of how regulation is accomplished in the presence of other nutrients (*curved magenta arrow*). In this work, we show that the reverse FruK reaction (*magenta arrow*) can also occur, providing a means to generate F-1-P from F-1,6-BP. Cra, catabolite repressor activator; F-1-P, fructose-1-phosphate; F-1,6-BP, fructose-1,6-bisphosphate; FruK, fructose-1-kinase.

the three key metabolites that regulate central metabolism, with F-1-P and F-1,6-BP presumably acting through their interaction with Cra (15).

One way to reconcile these observations would be if F-1,6-BP is converted to F-1-P. An obvious, although largely overlooked, means by which this could occur is *via* the "reverse" reaction of fructose-1-kinase (FruK; a member of ribokinase family (22); UniProt P0AEW9) (11, 23). To date, the only documented role for FruK is its "forward" reaction, which occurs after import/phosphorylation of exogenous fructose and uses ATP to convert F-1-P to F-1,6-BP and ADP (Fig. S2). However, all enzymes have the potential to catalyze their chemical reactions in both directions. Thus, we hypothesized that, if the reverse FruK reaction can occur under physiological concentrations (Table S1), then FruK can affect Cra's function by using F-1,6-BP derived from other carbon sources to generate F-1-P. Another intriguing possibility is that, since FruK was observed to directly interact with a chimeric protein containing the Cra regulatory domain ("LLhF"; Fig. S3) (24, 25), FruK might also directly interact with WT Cra and impact its activity.

In the study described herein, we assessed whether FruK carries out its reverse reaction, the potential for direct interactions between FruK and Cra, and contributions of FruK to *E. coli* metabolism. Our results suggest that FruK plays pleiotropic roles in *E. coli* that contribute to its bacterial physiology.

Results

FruK can generate F-1-P from physiological concentrations of F-1,6-BP and ADP

In determining whether FruK can use F-1,6-BP to generate Cra's strong allosteric regulator F-1-P, we first considered the *in vivo* concentrations of the metabolites involved in this catalytic reaction. The physiological concentrations of F-1,6-BP, ADP, and ATP were measured under a variety of growth conditions in at least two prior studies (15, 26). When *E. coli* are grown in the presence of glucose, F-1,6-BP can be as high as 15 mM and ADP is 0.55 mM (26) (Table S1).

In vivo concentrations of F-1-P are much more challenging to measure. Sample preparation can cause F-1,6-BP to spontaneously lose a phosphate, and F-1-P and F-6-P are difficult to distinguish without extensive separation (27, 28). To our knowledge, such measurements have not yet been widely implemented. Instead, the standard mass spectrometry measurement for F-1-P is to report its concentration relative to F-1,6-BP. When this ratio was reported for 43 different growth conditions (data from (15) replotted in Fig. S1), two conditions showed measurable changes: Exogenous fructose enhanced F-1-P and exogenous glucose-6-phosphate enhanced F-1,6-BP. The relative ratios for all other conditions correlated (albeit with large error bars for F-1-P), and it is difficult to determine which F-1-P results from enzymatic conversion, which might be confused with F-6-P and which arises from F-1,6-BP

breakdown during sample preparation. Finally, since Cra binds to F-1-P with micromolar affinities (7), only a low concentration must be catalytically generated in order to have an *in vivo* effect.

To determine whether FruK can carry out its "reverse" reaction (Fig. 1), the concentration of F-1,6-BP was titrated across the physiological range of 0.1 to 15 mM and ADP was fixed at 3 mM. Since the reverse reaction generates ATP, we monitored the reaction by coupling ATP formation to a luciferase assay. ATP generation was detectable in a concentration-dependent manner across a range of physiological F-1,6-BP substrate concentrations (Fig. 2), demonstrating that FruK can indeed generate F-1-P from F-1,6-BP. Similar results were obtained with both 27.5 nM and 275 nM FruK, both of which are well below the *in vivo* concentration of de-repressed FruK; the latter was estimated to be >2500 molecules per *E. coli* cell (25), which corresponds to a cellular concentration of 10^{-5} M (29).

Since we hypothesized that Cra and FruK can also directly form a protein–protein complex (described below), we tested if the presence of Cra would impact FruK activity. The addition of Cra, with or without DNA, had no significant impact on FruK activity.

FruK binds WT Cra in E. coli *crude cell extracts*

Our attention was first called to FruK in prior studies that used DNA pull-down assays to assess the functions of chimeric LacI/GalR homologs (25). In that study, FruK interacted with the LacI-Cra chimera "LLhF," which was composed of the DNA-binding domain of the *E. coli* lactose repressor protein (LacI) and the Cra regulatory domain (domain organization is illustrated in Fig. S3) but not with full-length LacI or other chimeras (25). This finding suggested that FruK could interact with the regulatory domain of WT Cra.

To test for the potential interaction between WT Cra and FruK, we again used a DNA pull-down assay. First, as a positive control, we repeated the experiment in which LLhF was over-expressed from a constitutive promoter and confirmed that it did indeed pull-down FruK when using immobilized $lacO^1$ operator (30) as a bait (Fig. 3*A*, lane 1). Next, we adapted the pull-down assay to use the consensus Cra DNA-binding site (O^{cra}) (2) as bait for constitutively over-expressed Cra. In this case, a band for Cra was readily identified, but no FruK was detected (Fig. 3*A*, lane 3). However, when fructose was added to the growth media (which would induce transcription of the *fruBKA* operon and thereby increase the levels of FruK protein (7)), a band for FruK was observed along with Cra (Fig. 3*A*, lane 6). Possible explanations for why LLhF does not require fructose in order to express high levels of the FruK protein are discussed in Supplemental Results. As negative controls, pull-down samples from strains that did not constitutively over-express Cra showed no Cra or FruK in either the absence or presence of fructose (Fig. 3*A*, lanes 5 and 7). Together, these data support the hypothesis that FruK binds directly to Cra.

In a complementary protein–protein pull-down experiment (*without* the addition of O^{cra}), His-tagged FruK from enterohemorrhagic *E. coli* (EHEC) was over-expressed in one bacterial culture and Flag-tagged Cra was over-expressed in another. When the two cell lysates were mixed, only two proteins were detected in the nickel-resin elution (Fig. 3*B*) and the identity of each band was confirmed by Western blot (Fig. 3*C*). These results suggest that the Cra–FruK reaction is specific and can occur in the absence of DNA.

FruK binds directly to Cra in vitro

Next, we directly examined the putative interaction between Cra and FruK using purified proteins and an adaptation of

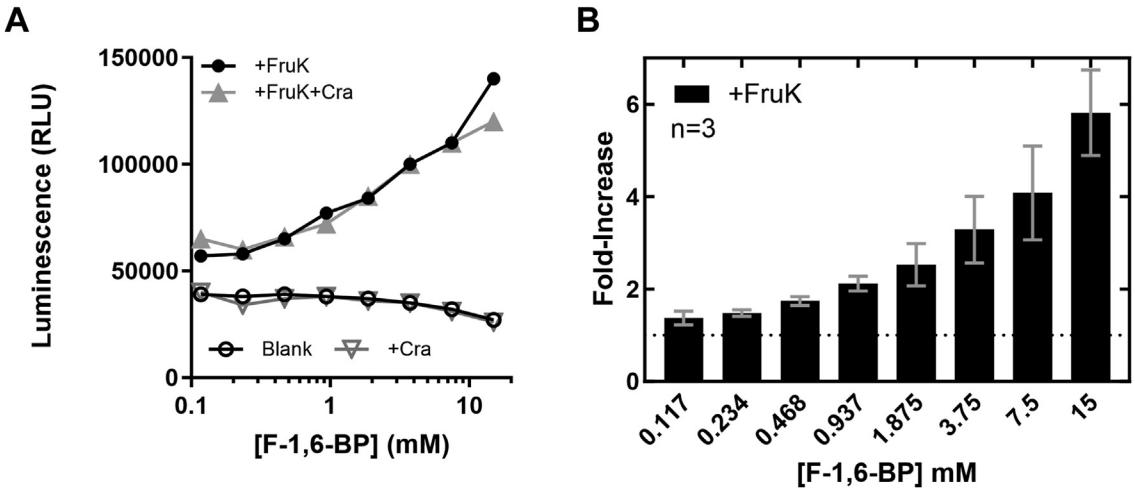

Figure 2. FruK generates ATP from ADP and F-1,6-BP. The "reverse" FruK reaction F-1,6-BP + ADP ← → F-1-P + ATP was coupled to a luciferase assay to detect the generation of ATP. The assays shown in these panels maintained constant concentrations of counter ions across the F-1,6-BP range. *A*, representative raw data for the luciferase reaction in the presence and absence of 275 nM FruK and/or 275 nM Cra. *B*, after normalizing to buffer-only controls, the average fold-increase in luciferase signal was calculated from three independent replicates of the +FruK luciferase assay at varied F-1,6-BP concentrations; error bars represent the SDs of the averages; two separate purifications of FruK were used for the three experiments. A fourth experiment using 27.5 nM FruK yielded statistically equivalent results. Cra, catabolite repressor activator; F-1-P, fructose-1-phosphate; F-1,6-BP, fructose-1,6-bisphosphate; FruK, fructose-1-kinase.

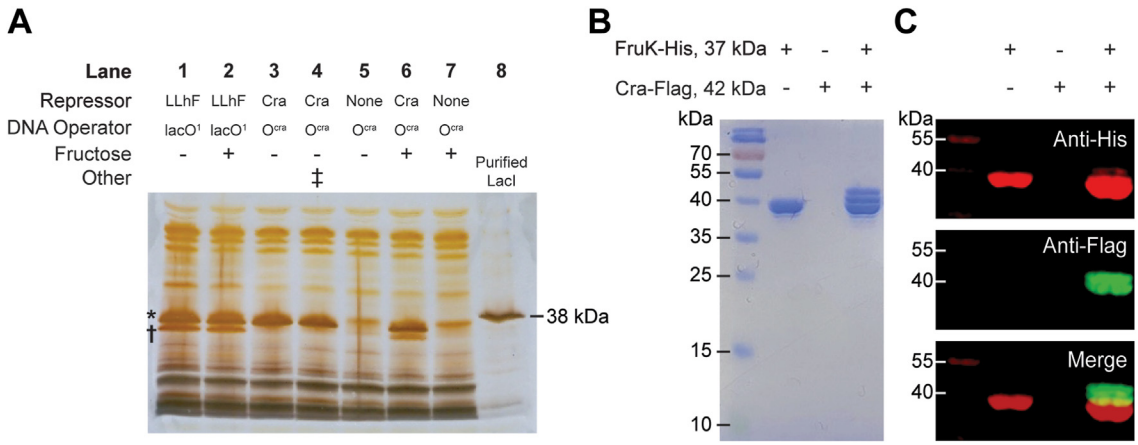

Figure 3. Cra forms complexes with FruK in *Escherichia coli* crude cell extracts. *A*, DNA pull-down assays using exogenous Cra and LLhF chimera show that both proteins interact with endogenous FruK. LLhF (lanes 1–2) and WT Cra (lanes 3, 4, and 6) were constitutively over-expressed in *E. coli* 3.300 cells; control cells (lanes 5 and 7) lacked exogenous repressor. All FruK was expressed from the genomic *fruBKA* operon. Cells were grown in MOPS media with glycerol as the carbon source, in either the absence (lanes 1 and 3–5) or the presence of 20 mM fructose (lanes 2 and 6–7). Lysed cells were incubated with the indicated immobilized DNA ($lacO^1$ or O^{cra}), and adherent proteins were visualized with SDS-PAGE and silver stain. The *asterisk* (*) indicates the position of the repressor (*top*), and the *dagger* (†) indicates the position of FruK (*bottom*); the identities of LLhF and FruK were previously ascertained with mass spectrometry. (24). In lane 4, the *double dagger* (‡) indicates that lysates from lanes 3 and 5 were mixed prior to the pull-down assay. In lane 8, purified *E. coli* LacI serves as a molecular weight marker: LacI (360 a.a.; 38,590 Da monomer; UniProt P03023) is slightly larger than Cra (334 a.a.; 37,999 Da monomer; UniProt P0ACP1), which in turn is slightly larger than FruK (312 a.a.; 33,756 Da monomer; UniProt P0AEW9). This result was shown in two independent experiments. *B* and *C*, protein pull-down assays from crude cell extracts with over-expressed and tagged Cra and FruK in the absence of exogenous operator DNA. Cell lysates prepared from BL21 (DE3) *E. coli* expressing FruK-His were mixed with those expressing Cra-Flag, then subjected to a pull-down assay using nickel-agarose beads and SDS-PAGE. Results shown represent three independent experiments. Protein detection was by (*B*) Coomassie staining and (*C*) Western blot; the row headers of panels *B* and *C* are identical. Eluted proteins were immunoblotted using anti-His (*red*, *top* panel) and anti-Flag (*green*, *middle* panel) monoclonal antibodies. The *lower* panel is an overlay. Note that FruK-His pulls down Cra of two different sizes. The smaller band likely corresponds to Cra that has lost its N-terminal DNA-binding domain (~50 amino acids). This domain is easily lost in Cra and other LacI/GalR proteins (95), most likely to proteolysis (96–98). The uncropped gels used to construct this figure are in Fig. S10. Cra, catabolite repressor activator; FruK, fructose-1-kinase.

biolayer interferometry ("BLI") (24) to quantify the interaction. We previously used this technique to quantify binding between purified FruK and the DNA-bound LLhF chimera; the binding affinity was $\sim 10^{-8}$ M (24). Also in this previously-published study, purified FruK did not bind to DNA-bound, purified LacI (24), again supporting the hypothesis that FruK's interaction with LLhF was mediated by its Cra regulatory domain rather than its LacI DNA-binding domain.

Here, we performed BLI equilibrium assays with purified full-length Cra and FruK; data from an example experiment at one FruK concentration are shown in Fig. S4. In these experiments, biotinylated O^{cra} DNA was immobilized to streptavidin fiber optic tips and then bound to purified Cra; this complex was then incubated with varied concentrations of FruK. Once equilibration was reached, the height of the signal plateau was plotted *versus* FruK concentration to generate titration curves (Fig. 4) (24). To calculate K_d from these curves, one must simultaneously determine the effective concentration of immobilized, DNA-bound Cra (24). This iterative process involved varying the amount of DNA-bound Cra that is immobilized on the tip, followed by global fitting of multiple independent experiments using the expanded equation for ligand binding (see Experimental procedures; Fig. 4). This analysis showed that the assay conditions were in the "intermediate" binding regime, that is, the concentrations of immobilized Cra-DNA were near the K_d for FruK binding $-2.0 \pm 0.5 \times 10^{-9}$ M. Notably, this value of K_d is several orders of magnitude below the concentration of FruK detected *in vivo* ($\sim 10^{-5}$ M when *fruBKA* is de-repressed; (25, 29)), which means that it is possible for the complex to form *in vivo*.

Since both WT Cra and the LLhF chimera interact with FruK with high affinity, we conclude that FruK indeed interacts with the regulatory domain(s) of Cra. Three control experiments indicate that this interaction is specific. (i) FruK alone did not bind to *fruB* DNA directly (Fig. S4, magenta). Neither Cra nor FruK bound to unrelated proteins, which rules out either protein being "sticky" and having promiscuous binding: (ii) As noted above, FruK did not bind full-length LacI (24); and (iii) DNA-bound Cra did not interact with *E. coli* pyruvate kinase, which is another metabolic kinase that is transcriptionally regulated by Cra (31) (Fig. S4).

Surprisingly, the affinity of FruK for full-length WT Cra was nearly ten-fold tighter than that determined for the LLhF chimera (24). Since FruK must bind to the regulatory domain that is common to both full-length Cra and the chimera (Fig. S3), the different binding affinities likely arise from long-range effects of their different DNA-binding domains. We envision two possible means by which could this occur: First, interactions between the alternative DNA-binding domains and the Cra regulatory domain could have long-range effects on FruK binding. Second, since the protein–protein binding affinity was measured in the presence of operator DNA, the different operators for the alternative DNA-binding domains (Cra *versus* LacI) could elicit different FruK-binding affinities *via* an allosteric mechanism.

Finally, we attempted to quantify FruK binding to full-length Cra in the absence of DNA by directly immobilizing either

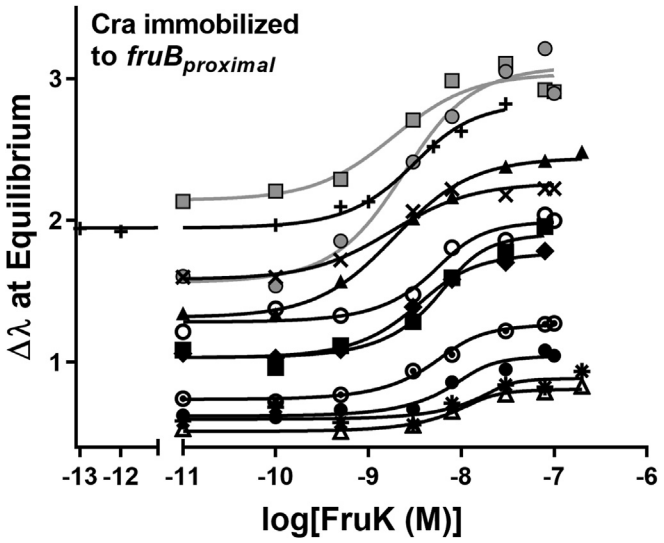

Figure 4. Purified FruK binds to immobilized, purified Cra/DNA. In these biolayer interferometry experiments, biotinylated DNA was immobilized to streptavidin-coated fiber optic tips and then incubated with a constant concentration of Cra (2.5 nM) and varied concentrations of FruK (x axis). The individual binding curves denoted with the varied symbols are from independent experiments that used four separate lots of purified Cra and six separate lots of purified FruK. Curves were generated by global fitting of these independent assays to Equation 2: K_d was common to all curves, whereas all other parameters were unique to each curve (*i.e.*, each curve had its own value of DT, Y_{max}, *etc.*). The variation in the Y axis intercept values arises from varied amounts of immobilized DNA; this variation is required in order to mathematically determine K_d (24) and either arose inherently due to differences among fiber optic tips (discussed extensively in (24)) or was deliberately varied by diluting biotinylated-DNA with free biotin prior to immobilization. The global fit for ten assays with untagged proteins (*black symbols/fit lines*) yielded a K_d of $2.0 \pm 0.5 \times 10^{-9}$ M. Including data for the His-tagged FruK (*gray circles* and *line*) in the global fit yielded a K_d of $2.1 \pm 0.4 \times 10^{-9}$ M; a similar result was obtained for His-tagged Cra ($1.6 \pm 0.4 \times 10^{-9}$ M; *gray squares* and *line*). Experiments were performed in 50 mM Hepes, 100 mM KCl, 0.1 mM EDTA, 10 mM $MgCl_2$, 0.3 mM EDTA, pH 7. Cra, catabolite repressor activator; FruK, fructose-1-kinase.

His-tagged Cra or His-tagged FruK to BLI tips. However, neither protein could efficiently bind the untagged partner; equilibrium was not reached after several hours. The impeded binding could be due to either the His-tag or immobilization on the tips. Since the tagged proteins functioned like non-tagged protein in other versions of the binding assay (*e.g.*, Fig. 4, gray symbols) and in cell lysate (Fig. 3, *B* and *C*), we conclude that direct immobilization of either Cra or FruK onto the BLI tip imposed steric constraints that impaired binding.

FruK dimer binds to a Cra dimer

To assess the stoichiometry of the Cra–FruK complex in the presence and absence of DNA, we used atomic force microscopy (AFM). This technique uses a cantilevered tip to measures the dimensions of individual molecules and complexes that have been deposited on a mica surface. Molecular volumes are then used to estimate molecular weights for each species. Prior to these experiments, the oligomerization state of unbound FruK was not known. Since its homolog ribokinase is a homodimer (32), we hypothesized that FruK would also be a dimer. The minimal functional unit of Cra is a homodimer, which has the capacity to bind one DNA operator (*e.g.*, (33–35)). The DNA for these experiments comprised a region of the *fruBKA* promoter that contains both the $fruB_{distal}$ and $fruB_{proximal}$ Cra operator sites; as such, one DNA had the potential to bind two Cra dimers.

Images of representative complexes are shown in Figure 5*A* and the complete AFM images are available at GitHub (https://github.com/ptoneil/2022_LSK_AFM_CraFruK.git). When the measured molecular volumes for the protein particles observed in the FruK+DNA and Cra+DNA samples were transformed into molecular weights, results corresponded very closely to the molecular weights expected for each homodimer (Fig. 5*B*); this provided confidence in the assumptions used for computations (36–38). The homodimeric Cra observed here differs from a previous report, in which purified Cra with a C-terminal His-tag appeared to be tetrameric (33); perhaps, these differences arise from different purification conditions.

Consistent with BLI results, FruK alone showed no binding to DNA (Fig. S5). As expected, Cra clearly bound to DNA (Fig. 5*A*), often causing a "kink" in the DNA that matched the 45 to 50° bend angle that occurs when LacI/GalR proteins bind to their cognate operator sites (*e.g.*, (39, 40)). Several instances were observed in which both operators on a single DNA were bound by separate Cra homodimers (*e.g.*, Fig. 5*A*).

When all three components (Cra, FruK, and DNA) were present in an AFM sample, the volumes of complexes ranged from that of (i) a single protein dimer "$(dimer)_1$," which could be either the Cra or FruK homodimer, (ii) to a dimer of protein dimers, "$(dimer)_2$," (iii) to a trimer of protein dimers, "$(dimer)_3$" (Fig. 5*B*). Model-free, one-dimensional clustering of these distributions identified (i) three distinct subpopulations of DNA-bound complexes, centered around $(dimer)_1$ (presumably Cra), $(dimer)_2$, or $(dimer)_3$ (Fig. 5*C*) and (ii) two-populations of DNA-free complexes, centered around $(dimer)_1$ (which could be either Cra or FruK) or $(dimer)_2$ (Fig. 5*D*). Due to the similar molecular weights of the Cra and FruK homodimers, as well as their overlapping distributions of measured volumes, the composition of $(dimer)_2$ and $(dimer)_3$ cannot be directly elucidated. However, we assumed that every DNA-bound complex must contain at least 1 Cra homodimer. Furthermore, since only homodimers were observed in the single protein samples, we deduced that the $(dimer)_2$ complex must contain one each of the Cra and FruK homodimers and that the $(dimer)_3$ complex must contain a mixture of Cra and FruK dimers.

Additional information about the possible stoichiometry of $(dimer)_3$ can be deduced from samples with varied protein concentrations (Fig. S6): The sample comprising 20 nM Cra/10 nM FruK had primarily $(dimer)_2$ and some $(dimer)_3$. When the FruK concentration was increased (20 nM Cra/20 nM FruK), the population of particles shifted to smaller complexes. Thus, we deduce that $(dimer)_3$ is Cra-FruK-Cra (each protein being a dimer) and that additional FruK saturated the Cra-binding sites limiting complex formation to $(dimer)_2$ Cra-FruK (Fig. S6).

Samples containing all three components (Cra, FruK, and DNA) also showed even larger complexes that were mostly absent from the Cra+DNA and FruK+DNA samples

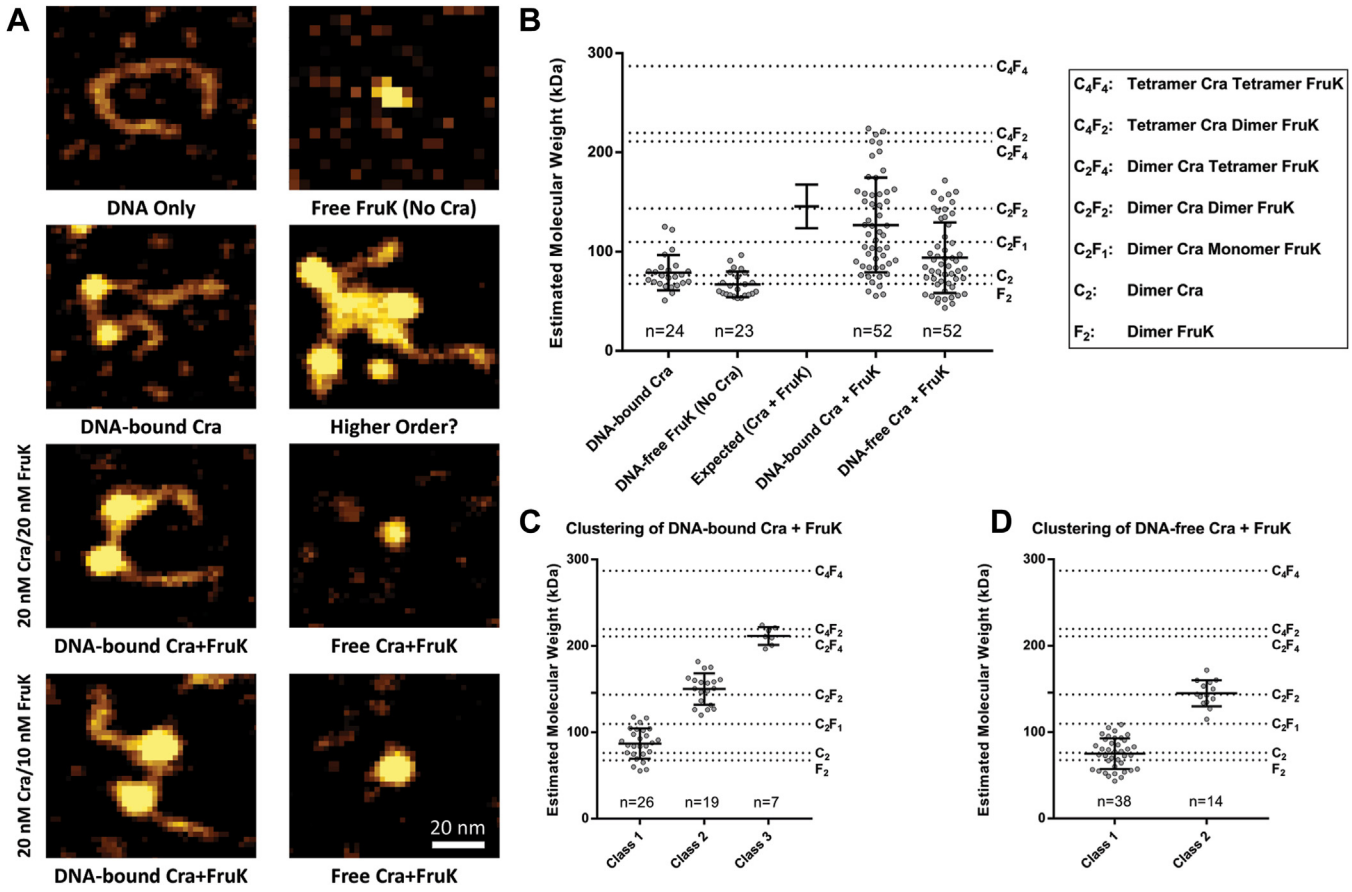

Figure 5. Distributions of Cra, FruK, and DNA complexes observed with atomic force microscopy. *A*, various combinations of DNA, Cra, and FruK were deposited on mica chips and scanned with AFM. The representative images shown represent 80 × 70 nm^2 sections of the scanned mica; complete images can be found online (https://github.com/ptoneil/2022_LSK_AFM_CraFruK.git). *B*, size distributions of observed protein complexes. Each dot on this graph represents a unique, measured peak in an AFM image; the bar represents the mean and SD for each population of dots. The number of individual complexes measured (n) is given above the x-axis. The dotted reference lines represent the expected molecular weights for various complexes. As another reference, values for the experimentally measured "DNA-bound Cra" and "Free FruK (No Cra)" were used to generate an "Expected (Cra + FruK)" value with propagated SD. The sample containing DNA, Cra, and FruK were combined from two independent samples, one with a Cra:FruK ratio of 2:2 and the other with a 2:1 ratio. Separate analyses of these two samples are in Fig. S6. *C*, the "DNA-bound Cra + FruK" population was well-fit using one-dimensional cluster analysis with a three-class system, fixing the upper class to n = 7. Other fitting attempts are descripted in Fig. S7. *D*, the "DNA-free Cra + FruK" population was well-fit using one-dimensional cluster analysis with two-classes. AFM, atomic force microscopy; Cra, catabolite repressor activator; FruK, fructose-1-kinase.

(*e.g.*, Fig. 6; other images available on GitHub). These were excluded from quantitative analyses based upon their size and complexity. While these larger complexes may represent nonspecific aggregation of Cra and FruK, the fact that all samples were made within minutes of each other and the single protein samples did not contain these complexes makes this unlikely. Rather, the presence of higher order oligomers raises the possibility that a FruK dimer may bridge Cra dimers (*i.e.*, $(dimer)_3$) to enable "looped" complexes with two or more DNA operators, similar to the dual-operator loops known to enhance repression by tetrameric LacI (*e.g.*, (25, 41–48)). Indeed, several of the Cra/FruK aggregates appear to include at least two DNA operators.

The absence of FruK impacts growth on a nonpreferred carbon source

If either the reverse FruK reaction (F-1,6-BP to F-1-P) or the direct interaction of FruK with Cra are biologically relevant, deleting FruK should have biological consequences when *E. coli* are grown on non-fructose carbon sources. Based on its potential to generate Cra's allosteric regulator F-1-P from the central metabolite F-1,6-BP, we hypothesized that abolishing expression of FruK protein would alter Cra's ability to regulate switching among the metabolic pathways that enable efficient use of alternative carbon sources. Indeed, an early report for a *fruK* mutant strain showed growth defects on lactate and a corresponding decrease in PEP-synthase (an enzyme required for gluconeogenesis (49) whose transcription is activated by Cra (50)).

For our growth experiments, we used the Δ*fruK724*::*kanR* strain from the Keio collection (51). To test whether FruK impacts growth on alternative carbon sources, we subcultured strains from M9/glucose media to M9 media with either glucose, glycerol, or fructose as the sole carbon source. In previous reports, ablation of fructose-1-kinase activity abolished *E. coli* growth on fructose (*e.g.*, (11)); thus, as a control experiment, we confirmed that the WT, but not the

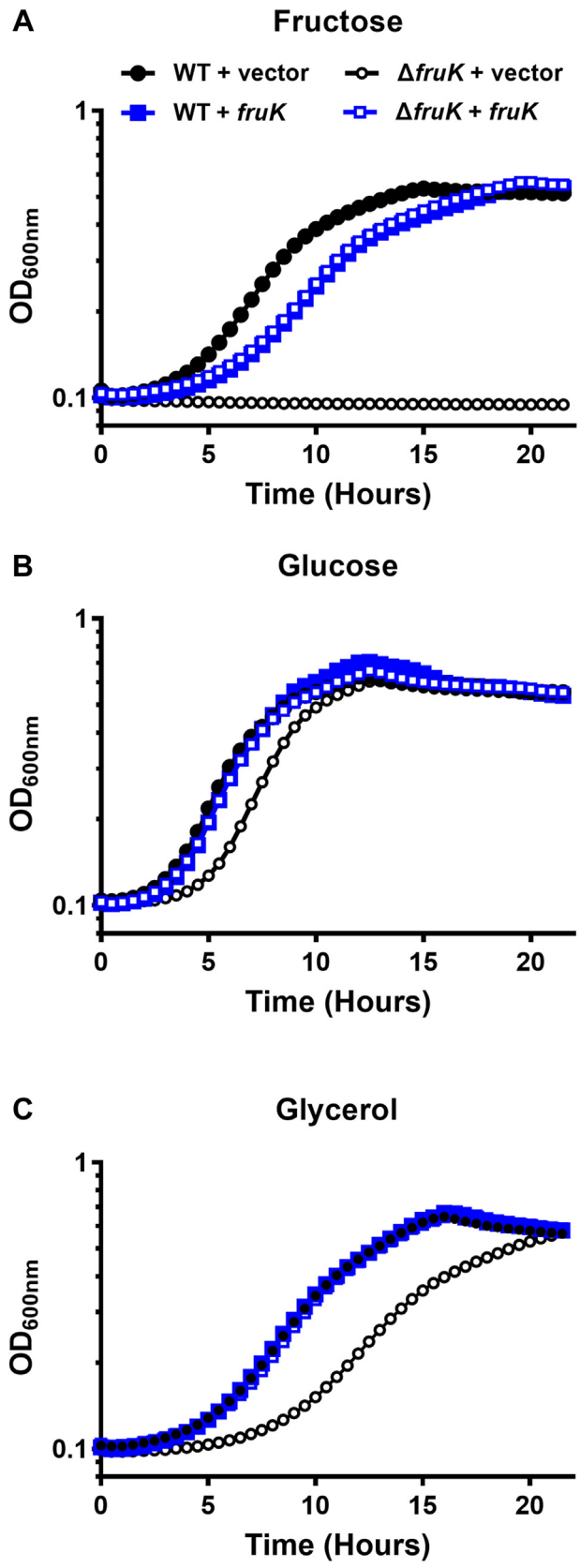

Figure 6. FruK contributes to *Escherichia coli* metabolism. Bacterial growth was measured for WT and Δ*fruK724*::*kanR* (Δ*fruK*) strains of *E. coli* transformed with pHG165a parent plasmid (vector) or pHG165a-FruK that constitutively expressed FruK (*fruK*). Cultures were grown in M9 minimal media containing either 0.2% fructose (*A*), glucose (*B*), or glycerol (*C*). OD_{600} was measured at 30-min intervals for 22 h. Symbols represent the mean with SD for n = 3 technical replicates; error bars are smaller than the symbols. The data shown are representative of three independent experiments, which were in good agreement with each other: For the uncomplemented Δ*fruK* strain relative to WT in media with glucose, the time required to reach half maximal OD_{600nm} was delayed by 0.5, 1.3, 1.7 h, respectively for the independent experiments; for media with glycerol, the time required to reach half maximal OD_{600nm} was delayed by 3.3, 3.4, and 3.8 h, respectively. Constitutive over-expression of FruK from a plasmid greatly reduced or abolished the delay time in all three experiments. Results in different growth conditions (Fig. S8) are in good agreement with the results shown here. Cra, catabolite repressor activator; FruK, fructose-1-kinase.

Δ*fruK724*::*kanR* mutant strain, was able to grow on fructose (Fig. 6*A* black). Growth on fructose was restored when FruK was constitutively expressed from a plasmid. Surprisingly, FruK expression on the multi-copy plasmid slightly inhibited growth on fructose in both the WT and Δ*fruK724*::*kanR* strains (Fig. 6*A*, open and filled blue symbols) relative to WT strain.

Next, we examined the ability of the strains to grow on the preferred carbon source, glucose (Fig. 6*B*). In this case, the Δ*fruK724*::*kanR* strain showed a slightly longer lag phase (Fig. 6*B*, open black symbols) relative to the other strains. This lag phenotype was reverted when FruK was provided on a plasmid (Fig. 6*B*, open blue symbols). Finally, we examined how the absence of FruK impacts growth on the nonpreferred carbon source glycerol (Fig. 6*C*). Under this condition, the Δ*fruK724*::*kanR* strain showed a pronounced lag phase (and somewhat slower growth rate) than the other samples (Fig. 6*C*, open black symbols); complementation with WT FruK again restored WT growth kinetics.

Thus, these results show that deleting FruK alters growth on glucose and glycerol, and this phenotype is exacerbated on the nonpreferred carbon source. In separate experiments, we examined the transition from Luria-Bertani broth to minimal media with different carbon sources for WT and the Δ*fruK724*::*kanR* strains. Similar to the other experiments, the absence of FruK led to a delayed in growth (Fig. S8), consistent with FruK playing a role in metabolic switching. These combined results are consistent with FruK playing a role in central metabolism that is beyond that of fructose metabolism.

Discussion

Although studied for decades, our understanding of how central metabolism is regulated in *E. coli* remains incomplete. Here, we considered that the little-studied enzyme FruK might play additional roles beyond that of fructose catabolism. Indeed, results for the growth assays showed that WT FruK plays a broader metabolic role, perhaps even contributing to metabolic switching that is known to be regulated by Cra. This phenotype might be accomplished by disrupting any (or several) of five different molecular mechanisms:

First, the reverse FruK reaction demonstrated herein (Fig. 2) generates the strong Cra allosteric inhibitor F-1-P from physiologically relevant concentrations of F-1,6-BP, thereby providing a metabolic pathway by which other sugars can be used to create F-1-P. The reverse reaction does not appear to

be influenced by interaction with Cra, suggesting that the FruK region implicated in Cra binding does not impact FruK catalysis.

Second, the nanomolar interaction observed between FruK and DNA-bound Cra is tight enough to exist *in vivo*. Cra and FruK have long been known to co-regulate each other's activities *via* transcription repression and F-1-P production, respectively (Fig. 1). The current results raise the intriguing possibility that the direct Cra–FruK interaction could also play an important biological role. If nothing else, the direct Cra–FruK interaction would produce F-1-P in the immediate vicinity of Cra. In addition, FruK binding to Cra might alter its ability to regulate transcription for specific operons. Since Cra directly regulates >40 natural operators, large scale studies will be needed to test this hypothesis. One means by which this could occur is through altering the binding affinity between Cra and a subset of its target operators.

Indeed, a third possibility is that the higher order Cra–FruK–DNA complexes observed in AFM could simultaneously bind and loop multiple DNA operators, similar to LacI's regulation of the *lac* operon (*e.g.*, (25, 41–46)). Consistent with this, six promoters in the Cra regulon have multiple Cra-binding sites (https://ecocyc.org/gene?orgid=ECOLI&id=EG10338#tab=REFS) (4, 5, 7, 52, 53). To test this hypothesis, additional experiments will require assays with longer inter-operator spacing than the current construct (54, 55).

A fourth possibility is that the Cra–FruK interaction could alter the Cra interaction with other transcription factors. Operon-specific interactions are known for EHEC Cra and KdpE (56), as well as for *E. coli* Cra and FNR (57). Fifth, for various Cra-activated pathways (such as those by which glycerol and lactate are metabolized), Cra-FruK binding could facilitate interactions with some other factor, such as RNA polymerase, as observed for members of the AraC/XylS family of transcription activators (*e.g.*, (58–60)).

Finally, we anticipate that FruK's newly discovered role(s) will vary with changing metabolic conditions. As noted above, *fruK* gene expression is itself regulated by Cra, leading to different cellular concentrations of FruK under different metabolic conditions. Such changes could alter whether the direct Cra-FruK complex is formed; indeed, this was likely detected in the *in vivo* pull-down assay first used to detect the Cra–FruK interaction (Fig. 3*A*; Supplemental Results). F-1,6-BP concentrations also depend upon available carbon sources (15, 26) (*e.g.*, Fig. S1 and Table S1). Effects of F-1,6-BP concentration changes on the reverse FruK reaction might resolve the conundrum as to how F-1,6-BP signals the need for altered metabolic flux. Thus, once the molecular mechanism(s) of FruK's contributions are elucidated, results should be used to improve current models of *E. coli* metabolic flux (15, 16, 21) to determine whether discrepancies with measured metabolites have been resolved.

In summary, the intriguing range of ways that FruK might co-regulate *E. coli*'s central metabolism will be important to further consider. As both Cra and FruK are conserved within the clade of γ-proteobacteria (*e.g.*, (8)), co-regulation by FruK could play a key role in a wide range of organisms.

Experimental procedures

Common reagents

The trisodium salt of D-fructose-1,6-bisphosphate (F-1,6-BP), ATP, and ADP were purchased from Sigma-Aldrich. For experiments, F-1,6-BP, ATP, and ADP nucleotides were dissolved in the appropriate buffer (detailed below) and the pH was adjusted to 7.0.

The barium salt of F-1-P was purchased from Sigma-Aldrich. To generate the more soluble sodium salt, Ba^{+} F-1-P was subjected to ion exchange chromatography to using a Dowex 50WX4 (Sigma) column pre-charged with 2 N HCl and equilibrated in ddH_2O. After several passages, the pH of the final eluant was adjusted to 7 with NaOH. Eluted F-1-P was lyophilized and used to make saturated stock solutions in ddH_2O. Concentrations of the stock solutions were determined by stoichiometric implementations of the enzyme assay, as reported previously (24).

The various operator sequences used are shown in Table 1. For pull-down, BLI, and filter-binding assays, DNA oligos were purchased from Integrated DNA Technologies. ssDNA was annealed using the protocol described in Swint-Kruse *et al.* (61). For pull-down assays and BLI, the purchased DNA oligos were 5' biotinylated. For filter-binding assays, annealed DNA was labeled with 32P-ATP (*e.g.*, (61)). For AFM, a 331 bp of *fruBKA* promoter, spanning both the $fruB_{distal}$– and $fruB_{proximal}$ binding sites, was amplified from the DH5α (F⁻ φ80*lac*ZΔM15 Δ(*lac*ZYA-*arg*F)U169 *rec*A1 *end*A1 *hsd*R17(r_K^-, m_K^+) *pho*A *sup*E44 λ⁻*thi*-1 *gyr*A96 *rel*A1) strain of *E. coli*. Further details of this reaction are described in the Supplemental Methods: Preparation of DNA for AFM.

Plasmid construction

Lists of bacterial strains and plasmids used in this work are in Table S2. The coding region for WT Cra (Supplemental Sequences) was amplified from Hfr(PO1), *lacI22, λ-, e14-,*

Table 1
Operator sequences used in Cra/FruK experiments[a]

Experiment	Name	Sequence (5' to 3')
Pull-down (biotinylated)	$lacO^1$	5'-BiosG-gcatatggcagcttgAATTGTGAGCGGATAACAATTttgcagacg
Pull-down (biotinylated)	O^{cra}	5'-BiosG-aatgcctgcatatggcagcttgaaGCTGAAACGTTTCAttttgcagcgatcgttac
Biolayer interferometry (biotinylated)	$fruB_{proximal}$	5'-BiosG-atgcatgttgtgtggTTCTTGAAACGTTTCAGCtcacacaggtcc
Atomic force microscopy	$fruB_{distal}$	5'-GAGGCTGAATCGTTTCAA
Atomic force microscopy	$fruB_{proximal}$	5'-TTCTTGAAACGTTTCAGC

[a] Sequences for the synthesized operators are shown in capital letters embedded in the common flanking sequence (lower case letters) for each type of technique. The sequences for $fruB_{proximal}$ and $fruB_{distal}$ are from (7). The consensus sequence O^{cra} is from (2). The sequence of $lacO^1$ is from (30).

relA1, spoT1, thiE1 E. coli (strain name 3.300; *E. coli* Genetic Stock Center, Yale University) using the primers 5'-ggtctccaggtgtgaaactggatgaaatcgc and 5'-gagctcttagctacggctgagcacgccgcgg. The gene was subcloned into the pHG165a plasmid using the procedure of Jones (62). Full gene sequencing showed that the coding region exactly matched that of UniProt P0ACP1. This plasmid has been deposited with Addgene (90066; plasmid name FruR-pHG165a).

An expression plasmid carrying the *E. coli fruK* gene on pET-3a was a gift from the Van Schaftingen laboratory at the Université Catholique de Louvain (23) (Addgene ID 186256). The FruK amino acid sequence was determined for this plasmid and is reported in Supplemental Sequences. Sequencing was performed by ACGT, Inc.

To generate pET3a-Cra-C-His, pET3a-N-His-FruK, and pET3a-FruK-C-His for BLI trials, plasmids expressing coding regions for untagged Cra and FruK were used as templates to amplify their respective genes, using two overlapping primers that include repetitive histidine codons (Table S3). The amplified products were digested with DpnI (New England Biolabs) to remove the parental plasmid before transformation into DH5-alpha *E. coli*. Positive clones were validated by gene sequencing. pET28a versions of EHEC FruK-C-His and EHEC Cra-C-Flag were generated by similar methods.

The ORF-encoding *E. coli* FruK was amplified from EHEC and cloned into pHG165a for constitutive, low-level expression (25) and subcloned into pET28a plasmid for inducible expression using the ABC cloning method (63). His-tagged versions were also created for pull-down assays. Primers used to generate pHG165a-FruK, pHG165a-FruK-C-His, and pET28a-FruK-C-His are listed in Table S3.

Analyses of reported FruK sequences

Upon sequencing the pET3a FruK expression plasmid, we found the coding region contained differences from the reported UniProt sequence (P0AEW9) (Supplemental Sequences). To assess whether the pET3a (or any other) FruK variant sequences occur naturally, we used the pET3a FruK sequence as the query in a BLAST search (64) of the nr database. The pET3a FruK sequence has 100% identity with each of the three sequences reported for *Salmonella* FruK. In addition, the sequences reported for *E. coli* FruK showed a range of mutations, including those observed in the pET3a/*Salmonella* sequence. To survey this range, BLAST results were filtered between 80 to 99.9 percent identity with query coverage between 85 to 100% of the FruK query. The resulting multiple sequence alignment was edited for aberrant sequences (generally comprising sequences with long N-termini or inserts of >20 amino acids). The remaining 364 sequences were aligned using clustalOmega (65) and analyzed with ConSurf (66) to assess the variability at each FruK position; 212 of the 312 positions showed some variability; only 100 positions were absolutely conserved. Several representative sequences are shown in Supplemental Sequences, including the FruK sequence on pET3a and that cloned from EHEC to pHG165 and pET28a. While sequencing errors are always possible, the frequency of observed changes leads us to conclude that *E. coli* FruK experiences natural variation.

Purification of FruK and Cra; verification of their activities

The procedure for purifying FruK was adapted from (23), as reported previously in the Supplementary Material to Weeramange *et al.* (24). In brief, 1 L cultures of BL21 (DE3) pLysS *E. coli* [F–, *omp*T, *hsd*S_B (r_B–, m_B–), *dcm*, *gal*, λ(DE3), pLysS, Cm^R, $[malB^+]_{K\text{-}12}(\lambda^S)$] carrying the FruK-pET-3a expression plasmid were grown to an OD_{600} of ∼0.6, at which time they were induced with 1 mM ITPG and grown for 44 to 45 h at 22 °C. After lysis in breaking buffer (20 mM potassium phosphate, 5 mM EDTA, 1 mg mL^{-1} lysozyme, 1 Pierce Protease Inhibitor Tablet (Thermo Fisher Scientific), 1 mM DTT, pH 7.4), FruK protein was purified with a two-step ammonium sulfate precipitation (using the supernatant from a 30% precipitation and the pellet from a 70% precipitation). The pellet was resuspended in buffer A (20 mM Hepes, 20 mM KCl, ½ tablet Pierce Protease Inhibitor A32963 from Thermo Fisher Scientific, 10% glycerol) and desalted with either (i) a Sephadex G25 column or (ii) by diluting the ammonium sulfate resuspension 1:5 with 20 mM KCl buffer A and then reducing the supernatant volume by half, using a Vivaspin MWCO 10 kDa concentrator (Sartorius Stedim Lab Ltd) and centrifugation with a Sorvall HB-6 rotor (Thermo Fisher Scientific) at 5500 rpm (4900*g*) for 12 to 15 min at 4 °C. The latter performed better in the following subsequent DEAE ion exchange chromatography. For anion exchange, a two-step gradient was used to elute the FruK: (i) 20 to 250 mM KCl in buffer A and (ii) 250 to 500 mM KCl in buffer A. FruK protein elutes near the end of the first gradient. The identity of the purified FruK protein was confirmed by mass spectrometry by the KUMC Mass Spectrometer/Proteomic Core.

Aliquots of eluted FruK were stored in 30% glycerol at −80 °C. Glycerol is a key buffer component. If this osmolyte was removed by dialysis, FruK enzymatic activity decayed over the course of 30 min – 1 h. Prior assays indicated that part of the FruK elution peak was contaminated with a small molecule that inhibits various FruK functions. Thus, immediately prior to each assay, this contaminant was removed by diluting the protein to ≤3.5×10^{-3} mg mL^{-1} (∼100 nM) with FruK exchange buffer (20 mM Hepes, 40 mM KCl, 1 mM EDTA, 20% glycerol, 0.3 mM DTT) and re-concentrating it with a Vivaspin MWCO 10 kDa; dilution and concentration was carried out 3 times in total. The final protein concentration was determined with a Bradford assay (Bio-Rad Laboratories, Inc) and is reported as molar dimer. The enzymatic activity of the purified protein was verified using the reaction designed for the forward enzymatic reaction, as previously reported (24).

The protocol to purify WT Cra was similar to that used to purify lactose repressor protein (LacI) and LLhF (24, 61, 67–70). *E.coli* B *omp*T, *hsd*$S_B(r_B^- m_B^-)^-$, *gal, dcm, lac* cells (strain name "BLIM" (71)) were transformed with plasmid constitutively expressing WT Cra and grown in 6 L 2xYT media for 19 h at 37 °C; for some preps, growth media included 1% fructose, but this did not appear to alter either the

amount or activity of the purified Cra. After pelleting by centrifugation at 676*g* for 20 min and 4 °C, the cells were resuspended in ∼50 ml breaking buffer (0.2 M Tris–HCl, 0.2 M KCl, 0.01 M $MgCl_2$, 1 mM DTT, 5% glucose, pH 7.6) with 20 mg lysozyme and half of a crushed Pierce Protease Inhibitor Tab (Thermo Fisher Scientific) and frozen at −20 °C. All subsequent purification steps were carried out on ice or at 4 °C.

Cell lysis was accomplished by thawing the cell pellet on ice with breaking buffer added to a final volume of 150 ml and another crushed protease tab. At this step, the addition of 120 mg extra lysozyme was critical for chaperoning the Cra through ammonium sulfate precipitation, which was an unexpected activity of lysozyme. After lysis, 240 µl of 80 mg mL^{-1} DNase I from bovine pancreas (Roche Diagnostics) was added along with $MgCl_2$ to a final concentration of 30 mM. The crude cell extract was cleared by centrifugation at 9700*g* (8000 rpm) for 50 min at 4 °C prior to 23% ammonium sulfate precipitation (Thermo Fisher Scientific). The technical aspects of ammonium sulfate precipitation were very important. The chemical must be finely ground and lightly salted over the whole surface of the solution (generally 180–200 ml in a 400 ml beaker) at a rate so slow that crystals never reach the bottom of the flask. The mixture was allowed to precipitate for 30 min at 4 °C with slow stirring prior to centrifugation at 9700*g* (8000 rpm) for 40 min and 4 °C.

After precipitation, the pellet was gently resuspended in 50 ml cold 0.05 M KP buffer (KP buffer comprises potassium phosphate at the indicated molarity, 5% glucose, 0.3 mM DTT, pH 7.5) and dialyzed in regenerated cellulose Fisherbrand Dialysis Tubing (MWCO 12,000-14,000) against 1 L of cold 0.05 M KP buffer for 30 min, with three buffer changes. The dialysate was cleared by centrifugation, diluted 1:6 with 0.05 M KP buffer, and loaded onto a phosphocellulose column (Whatman P11) that was pre-equilibrated in 0.05 M KP buffer. The Cra protein eluted shortly after the beginning of a 0.05 M to 0.2 M KP buffer gradient, which was benchmarked against LacI variants as behaving like a dimer (61, 72). Purity was assessed on SDS-PAGE with silver stain and was estimated to be >90% (*e.g.*, Fig. S2 in (73)). The pre-column dilution (1:6 in 0.05 M KP buffer) was key to good purity; without it, Cra eluted from the phosphocellulose column much later and was contaminated with lysozyme and other proteins. Purified Cra was aliquoted and stored at −80 °C. Protein concentration was determined by Bradford assays (Bio-Rad Laboratories, Inc) and was generally 0.1 to 0.2 mg mL^{-1}. DNA activity assays (74) using the filter-binding technique (below) were used to assess the fraction of purified Cra that was active; preparations were generally 70 to 90% active.

Note that the concentrations of purified FruK and Cra are given in terms of molar dimer for all assays.

FruK reverse reaction

The forward reaction of purified FruK was detected by coupling ADP formation to the activities of pyruvate kinase and lactate dehydrogenase, ultimately assessing the change in NADH concentration (*e.g.*, Fig. S2) (24). To detect the formation of ATP during the reverse reaction, we used the Kinase-Glo kit (Promega, V6728) to assess the activity of purified FruK.

To maintain both good buffer capacity and a constant ionic strength across all substrate concentrations, stock solutions of trisodium F-1,6-BP (Sigma-F6803) and monosodium ADP (Sima-A2754) were made in Cra1X base buffer (50 mM Hepes, 0.1 KCl, 0.1 EDTA, 10 mM $MgCl_2$, pH 7). ATP (Sigma A9187) for controls were diluted in buffer containing Cra1X base buffer with 115 mM NaCl and 2 mM $MgCl_2$. All substrate solutions were adjusted to pH 7.0. Assay dilutions were performed with Cra1X base buffer with 180 mM NaCl, 40 mM KCl, and 10 mM $MgCl_2$. The final ion concentrations in the assay wells were 66.6 mM K^+, 95.5 mM Na^+, 10 mM Mg^{2+}, and 105 mM Cl^-. The experiment shown in Figure 2 also included 275 nM "washed" Cra.

Triplicate technical replicates for each substrate concentration were prepared in Costar white 96 well plates as follows: Each well contained either (i) 60 µl of the FruK reaction sample and 50 µl Kinase-Glo reagent for a total volume of 110 µl or (ii) 60 µl of ATP at varying concentrations plus 50 µl of Kinase-Glo reagent for a total of 110 µl. The final FruK and Cra concentrations were maintained at 275 nM, ADP was 5.5 mM, F-1,6-BP ranged from 0.1 to 15 mM, and ATP controls ranged from 0.03 to 4 mM. For reactions that included Cra or DNA, these components were included in the dilution cocktail used for serial dilutions of F-1,6-BP. After incubating for 1 h (shorter times produced lower signals), luminescence was read at room temperature using a SpectraMax M5 plate reader at all wavelengths.

Control reactions showed that that increasing the ionic strength inhibited activity of luciferase, making it critical to balance the counter ions of the changing substrate concentration (Fig. S9). Luciferase assays of the FruK forward reaction to monitor the disappearance of ATP did not detect enzyme activity. Since the forward reaction was readily detected in a different assay (Fig. S2), we concluded that either (i) the conditions needed to balance ionic strength across the titration of the forward reaction was even more inhibitory to the luciferase reaction and/or (ii) reagents in the luciferase reaction inhibited the FruK forward reaction.

DNA pull-down assay with WT Cra and endogenous FruK

For pull-down assays, the pHG165a plasmid encoding WT Cra (Addgene ID 90066) was transformed into the *E. coli* strain 3.300 (genotype Hfr(PO1), *lacI22, λ-, e14-, relA1, spoT1, thiE1*). Cultures were grown at 37 °C to saturation in 3 ml of MOPS media (Teknova: 40 mM morpholinopropanesulfonic acid, 10 mM NH_4Cl, 4 mM tricine, 50 mM NaCl, and other trace metals listed for product number M2101) supplemented with 0.8% glycerol, 1.32 mM dibasic potassium phosphate, 10 mM $NaHCO_3$, 0.2% casamino acids, 0.0025% thiamine, and 100 µg mL^{-1} ampicillin (75, 76). Cells were pelleted by centrifugation, resuspended in 100 µl breaking buffer (0.2 M Tris–HCl, 0.2 M KCl, 0.01 M $MgCl_2$, 1 mM DTT, 5% glucose,

ASBMB

pH 7.6) and lysed *via* freeze-thaw with 40 μl of 5 mg mL^{-1} lysozyme. Crude cell lysates were clarified by centrifugation. Ten (10) microliters of supernatant were incubated with biotinylated DNA that was immobilized to streptavidin magnetic beads (1 pmol DNA to 1 μl beads; New England Biolabs), as described in Meinhardt *et al.* (77). Sequences of the biotinylated DNA operators (Integrated DNA technologies) are listed in Table 1. After washing in FB buffer (10 mM Tris–HCl, 150 mM KCl, 10 mM EDTA, 5% DMSO, 0.3 mM DTT, pH 7.4), the protein-DNA beads were resuspended in 15 μl of denaturing buffer (10 μl 20% sodium dodecyl sulfate plus 5 μl 1M DTT). Adherent proteins were visualized with SDS-PAGE.

In prior pull-down assays with engineered LLhF, the second, slightly smaller band was identified with mass spectrometry to be FruK (24). These experiments were carried out using the now-discontinued Phast-gel 10 to 15% gradient, (GE Healthcare; former catalog #: 17-0540-01) to resolve the repressor protein band from the FruK band.

Results are in Figure 3*A*. The uncropped gels associated with this Figure are in Fig. S10.

Pull-down assay with over-expressed FruK and Cra

BL21 (DE3) *E. coli* (Novagen) carrying a modified pET28a expressing either EHEC FruK-C-His or EHEC Cra-C-Flag were grown in 150 ml LB supplemented with kanamycin (50 μg mL^{-1}) to an OD_{600} of 0.5. Protein over-expression was induced with IPTG (0.5 mM) for 4 h at 30 °C. After centrifugation, the bacterial pellet was suspended in 4 ml of 50 mM sodium phosphate, pH 8.0, 0.5 mg mL^{-1} lysozyme and incubated on ice for 30 min. An equal volume of 50 mM sodium phosphate, pH 8.0, 2 M NaCl, 8 mM imidazole, 20% glycerol, and 0.5% Triton X-100 was added. After 30 min on ice, the bacterial lysate was sonicated and then clarified by centrifugation.

For the pull-down assay, equal amounts (200 μl) of FruK and Cra cell lysates were mixed with 100 μl of nickel-nitrilotriacetic acid beads (Qiagen). After overnight incubation at 4 °C with gentle rotation, mixtures were loaded on a Poly-Prep Chromatography Column (Bio-Rad) and washed with 5 ml of 50 mM sodium phosphate, pH 8.0, 600 mM NaCl, 10% glycerol, 60 mM imidazole. Adherent proteins were eluted in 50 mM sodium phosphate, pH 8.0, 600 mM NaCl, 10% glycerol, and 250 mM imidazole.

Elution samples were subjected to SDS-PAGE on a 15% acrylamide gel (Supplemental Methods: SDS-PAGE) stained with Coomassie Brilliant Blue R-250. These gels were made using the original method of Laemmli (78). Aside from the Phast-gel used in the DNA-pull-down experiments (described above), no other commercial acrylamide gels tested to date have been able to resolve Cra from FruK due to their similar molecular weights. Western blot analysis used anti-His (Santa Cruz Biotechnology sc-8036; mouse) and anti-Flag (Sigma F7425; rabbit) as the primary monoclonal antibodies. Secondary antibodies were purchased from Li-Cor (goat anti-mouse IRDye 680RD and goat anti-rabbit IRDye 800CW). Western blots were imaged using a Li-Cor Odyssey at 680 and 800 nm.

Results are in Figure 3, *B* and *C*. The uncropped gels associated with this Figure are in Fig. S10.

Biolayer interferometry

In BLI, macromolecules are immobilized to a fiber optic tip, which can then be dipped into solutions of other macromolecules. Changes to the thickness of the bound layer (*e.g.*, when a second protein binds the immobilized macromolecule) are detected by a change in reflectance when light is passed through the tip (79). BLI was originally devised to measure the on and off rates of kinetic assays and thereby quantify binding affinities (80); we previously adapted BLI to measure binding affinities under equilibrium conditions (24). This adaption was required because the kinetic association curves for the Cra homologs LacI and LLhF were multiphasic (24); furthermore, dissociation curves could reflect both dissociation of FruK from Cra and dissociation of Cra from DNA. The equilibrium implementation was used here to measure FruK binding to DNA-bound Cra, using an Octet RED96 (Forté Bio, Pall Life Sciences; Fig. 4).

For FruK binding to DNA-bound Cra, experiments used "High-Precision Streptavidin" probe tips (Forte Bio) to which various biotinylated DNA sequences were attached (Table 1). Tips were first hydrated for at least 10 min in the DNA immobilization buffer (50 mM Hepes, 0.1 M KCl, 0.1 mM EDTA, 10 mM $MgCl_2$, pH 7.0, 0.3 mM DTT with 0.1 mg mL^{-1} BSA), loaded with biotinylated DNA (120 s), washed in immobilization buffer (30 s), and then dipped into pre-equilibrated solutions of 2.5 nM Cra dimer plus varied concentrations of FruK. Immobilization buffer was similar to the PYK buffer used in the FruK enzyme assay. For DNA loading, immobilization buffer contained 80 nM DNA. Protein solutions were kept on ice until added to final reaction tube, which was then allowed to warm to room temperature (~15 min; BLI signals are highly temperature-dependent.) All BLI steps were carried out with shaking at 2200 rpm.

The signal changes associated with protein binding were monitored as a function of time until a plateau was reached. Experiments were repeated on separate days with different Cra and FruK preparations. The FruK could contribute up to ~ 1/15th of the final reaction volume; because the FruK storage buffer differed significantly from the Cra storage buffer and contained 20% glycerol, we performed control experiments comprising Cra (i) pre-incubated with equivalent volumes of FruK storage buffer and (ii) with added glycerol; no effects were observed on DNA binding. Prior control experiments showed that FruK alone did not bind immobilized DNA (Fig. S11 in (24)).

As extensively discussed in prior publications (24, 74), any equilibrium binding event should be assessed to determine whether it is in the "stoichiometric" binding regime, the "equilibrium" binding regime, or intermediate between the two. The feature that differentiates these regimes is the relationship of the fixed component of the binding reaction (here, immobilized Cra-DNA) to the K_d for the binding event. If (and only if) the concentration of the fixed component is at least

10-fold less than the K_d value, the binding event falls in the equilibrium regime, and K_d can be determined by fitting the binding curve with Equation 1, which is derived using several simplifying assumptions:

$$Y = c + Y_{max} * \frac{10^X}{K_d + 10^X} \quad (1)$$

If the fixed component is not at least 10-fold below K_d, then the binding reaction is in either the "stoichiometric" or "intermediate" regime and fits should use Equation 2 (81):

$$Y = c + Y_{max} * \frac{\left(n + \frac{10^X}{DT} + \frac{K_d}{DT}\right) - \left(\left(n + \frac{10^X}{DT} + \frac{K_d}{DT}\right)^2 - 4n * \frac{10^X}{DT}\right)^{0.5}}{2n} \quad (2)$$

In both Equations 1 and 2, "Y" is the observed signal, "c" is the baseline value when the concentration of protein is zero, "Y_{max}" is the signal observed at saturation, "X" is the log of the FruK concentration (transformed to improve data point weighting in nonlinear regression), and "K_d" is the equilibrium dissociation constant. In Equation 2, "n" is the stoichiometry of the complex (here, n is assumed to 1) and "DT" is the total concentration of the species at fixed concentration.

The large number of parameters in Equation 2 requires global fitting of multiple experiments to ascertain a reliable estimate of K_d. In the BLI assays, we previously ascertained that the effective concentration of immobilized DNA (and therefore of DNA-bound Cra) is $\sim 10^{-9}$ M (24). Thus, for binding events with K_d values $< 10^{-8}$ M, titration curves should be fit with Equation 2. Since the K_d value is not known at the start of an experiment, the binding regime must be determined from the shape of the binding curve and the effects of varying the fixed component (here, the concentration of immobilized DNA/Cra) in the binding reaction. For the Cra–FruK interaction, these processes revealed that the affinity was in the intermediate regime, with a K_d of $2.0 \pm 0.5 \times 10^{-9}$ M (Fig. 4).

A second implementation of the BLI assay attempted to measure FruK binding to DNA-free Cra, using His-tagged Cra and FruK immobilized to Ni-NTA Dip and Read Biosensors (Forté Bio 18-5101; see Supplemental Results).

Atomic force microscopy

For AFM, a support substrate of freshly cleaved mica was functionalized with a 167 μM solution of 1-(3-aminopropyl)-silatrane, as described previously (82). Cra and FruK protein samples were mixed with DNA at the indicated concentrations in 1× Cra Buffer (50 mM Hepes, 100 mM KCl, 0.1 mM EDTA, 10 mM $MgCl_2$, 0.3 mM DTT, pH 7.0) and incubated for 60 min at room temperature. After incubation, a 1:4 dilution of each sample was made using 1× Cra Buffer, of which 9 μl were immediately deposited on the functionalized mica surface. Deposited samples were incubated for 2 min, then rinsed with 200 μl ddH_2O and dried with a gentle stream of argon. A typical image of 1 × 1 μm^2 with 512 pixels/line was obtained under ambient conditions with a MultiMode AFM system (Bruker) using TESPA probes (Bruker Nano) housed at the Nanoimaging Core Facility at the University of Nebraska Medical Center. AFM images available to download from GitHub with the analyzed complexes indicated with boxes.

To analyze the particles observed in the AFM images, the volume of DNA-bound and DNA-free protein complexes were measured using AtomicJ (83). The profile tool was used to obtain the following measurements: the complex height (h), the width at half-height of the long axis (w_{long}), and the width at half-height of the orthogonal axis (w_{orth}). For DNA-bound complexes, the height (h_{DNA}) and width at half-height (w_{DNA}) were also obtained for DNA adjacent to each DNA-bound complex. To calculate the volume (V) from the AFM images, peaks corresponding to protein complexes were fit as an elliptic cylinder

$$V = \pi * h * r_{long} * r_{orth} \quad (3)$$

with the radii (r_{long} and r_{orth}) being half of the measured widths. DNA was considered to be a cylindrical segment:

$$V = 2/3 * h_{DNA} * W_{DNA}^2 \quad (4)$$

For DNA-bound complexes, the volume of adjacent DNA was subtracted so that only the volume attributed to the protein(s) remained. (Two other geometric models were considered for the protein peaks, but neither could be matched to the expected molecular weights: (i) Treating the peaks as a segment of a sphere under-estimated the volumes compared to expected molecular weights. (ii) Treating the peaks as a rectangular box over-estimated the volumes compared to expected molecular weights.).

To convert volumes to molecular weight, the nm^3 volumes were divided by a conversion factor for the density. A value of 0.67 ml/g was determined from the crystal structures of both the Cra regulatory domain (PDB 2IKS; (34)) and ribokinase (PDB 1RKA (84); ribokinase is a homolog of FruK). The density values were obtained by dividing the solvent-excluded volume (calculated by the *surface* command within UCSF Chimera (85)) by the molecular mass of the atoms present (mass for missing residues was subtracted). On the plots, reference lines for higher order complexes were calculated from the theoretical molecular weights for monomeric Cra (37,999 Da) and monomeric FruK (33,756 Da).

*Growth curves of WT and Δ*fruK E. coli

To detect the biological outcomes of *fruK* deletion, we performed growth assays with the parent strain BW25113 (F-, *Δ(araD-araB)567, ΔlacZ4787*(::rrnB-3), *λ-, rph-1, Δ(rhaD-rhaB)568, hsdR514*) and its isogenic *ΔfruK724::kanR* mutant JW2155-1 from the Keio collection (51) that were obtained from the *E. coli* Genetic Stock Center at Yale University. To confirm the disruption of *fruK* in JW2155-1, the following primers were designed to flank the *fruK* gene (NCBI gene ID:

BW25113_RS11315; WP_000091263.1): fwd 5'-agcagcagcgttttcattatg-3'; rev 5'-gacgctatcgctgctgg-3'. NEB Q5 High-Fidelity polymerase was used in a standard PCR reaction, and the transposon disruption of *fruK* resulting amplicons was confirmed by sequencing (ACGT).

In addition, whole genome Illumina sequencing was carried out by Microbial Genome Sequencing Center LLC. Results verified that the WT Keio strain had the expected genotype with no novel substitutions. The genome for the Δ*fruK* Keio strain confirmed the *fruBKA* deletion and showed two point mutations relative to the WT strain. Both led to single amino acid substitutions in protein-coding regions: D602G in the "putative alpha-glucosidase" *yicI* and R214P in the transcriptional regulator *lrhA*.

Literature searches on *yicI* showed that this gene encodes an alpha-xylosidase (86) that "preferentially removes the xylosyl residue from the glycosyl residue of non-galactosylated oligosaccharides" that are common in plant cell walls and seeds (87). Δ*yicJI* showed decreased stationary phase on LB and fitness effects when co-inoculated with a WT strain in a variety of growth conditions with agitation (88). However, this phenotype does not match our Δ*fruK* delayed growth phenotype on glycerol (which eventually reaches the same level as the stationary phase of WT) nor would we expect this defect to be complemented by the FruK-expressing plasmid that we observed. Thus, we conclude that this mutation is unlikely to be the source of the delayed growth on glycerol that we report for the Δ*fruK* strain (Fig. 6).

Literature searches on *lrhA* showed that this gene encodes a negative transcription regulatory protein that controls flagellar, motility, and chemotaxis genes. No studies were found that showed effects of this gene on bacterial growth. If mutations in *lrhA* did alter growth, we would not expect it to be complemented by the expression of FruK protein (Fig. 6).

pHG165a (vector) and pHG165a-fruK (from EHEC) were transformed into BW25113 (WT) or Δ*fruK724*::*kanR* (Δ*fruK*). Strains were grown overnight in "M9" minimal media (48 mM sodium phosphate, 22 mM potassium phosphate monobasic, 18.7 mM ammonium chloride, 8.5 mM sodium chloride, 2 mM magnesium sulfate, 0.1 mM $CaCl_2$) supplemented with 0.2% glucose and ampicillin (100 ug mL^{-1}) at 37 °C with 250 rpm. The following day, cultures were pelleted at 4500*g* using the Sorvall ST 16R Centrifuge for 10 min then washed twice with M9 minimal media with no carbon source added. The cells were then resuspended in M9 minimal media with no carbon source. The optical density was taken at a wavelength of 600 nm using Genesys 10S UV-Vis Spectrophotometer and adjusted to OD_{600} = 0.025 in 1 ml of M9 media with either 0.2% glucose, fructose, or glycerol supplemented with ampicillin (100 μg mL^{-1}). These suspensions were then transferred into a nontreated 96-well plate in triplicate with 200 μl per well and incubated for 24 h in a Tecan plate reader at 37 °C with orbital shaking. A600 readings were taken every 30 min.

A second version of the growth assay was modified from the protocol of Hall *et al.* (89) and used uncomplemented cells with switching from LB to M9 media supplemented with 9 mM $MgCl_2$. These Methods and Results are reported in Fig. S8. Results from the two implementations of the growth assay are in good agreement.

Data availability

The original AFM data files, a PDF identifying the analyzed particles, a copy of the AFM methodology, and an Excel file of the measurements collected are available online *via* GitHub: https://github.com/ptoneil/2022_LSK_AFM_CraFruK.git; all other data are in the main manuscript or the supplement.

Supporting information—This article contains supporting information (90–94).

Acknowledgments—We thank the following KUMC scientists for their assistance with this work: Dr Dipika Singh (initial FruK enzyme assays), Dr Max S. Fairlamb (initial BLI assays), Mr Benjamin F. Rau (assistance in the early stages of the project); and Dr Alexey Ladokhin (English translation of (49)). We thank the van Schaftingen laboratory for the gift of the *fruK* expression plasmid. Drs Yuri Lyubchenko and Alexander Lushnikov at University of Nebraska Medical Center Nanoimaging Core Facility provided assistance with the AFM.

Author contributions—C. W., S. E. Q., S. S., P. R. H., A. W. F., J. L. B., and L. S.-K. conceptualization; C. W., C. M., P. T. O., S. E. Q., K. S. H., S. M., C. L. B., S. S., and P. R. H. formal analysis; C. W., C. M., P. T. O., S. E. Q., K. S. H., S. M., C. L. B., S. S., P. R. H., and P. S. H. investigation; C. W., C. M., P. T. O., and L. S.-K. visualization; C. W., C. M., P. T. O., S. E. Q., P. R. H., A. W. F., J. L. B., and L. S.-K. writing–original draft; C. M., P. T. O., S. E. Q., P. R. H., A. W. F., P. S. H., J. L. B., and L. S.-K. writing–review and editing; P. R. H., A. W. F., P. S. H., J. L. B., and L. S.-K. funding acquisition; S. E. Q., S. S., P. R. H., A. W. F., J. L. B., and L. S.-K. methodology; C. W., C. M., P. T. O., S. E. Q., K. S. H., S. M., C. L. B., S. S., and P. S. H. data curation.

Funding and additional information—This project was supported by the National Institute of General Medical Sciences at the National Institutes of Health by the following grants: the Center for Biomedical Research Excellence in Protein Structure and Function (P30 GM110761) to L. S. K., R01 GM079423 to L. S. K., P20 GM130448 to P. R. H., and P20 GM113117 to P. S. H. This research was also supported by funding from the National Institute of Allergy and Infectious Diseases awards R01AI121073 and R21AI153773 to J. L. B. and by private funds. The content is solely the responsibility of the authors and does not necessarily represent the official views of the National Institutes of Health.

Conflict of interests—During the course of this work, Dr Bose served on the Scientific Advisory Board and was a consultant for Azitra, Inc and Merck & Co, Inc. These activities did not financially support and are unrelated to the current manuscript. The other authors declare that they have no conflicts of interest with the contents of this article.

Abbreviations—The abbreviations used are: AFM, atomic force microscopy; BLI, biolayer interferometry; Cra, catabolite repressor activator protein; EHEC, enterohemorrhagic *Escherichia coli*; F-1,6,-BP, fructose-1,6,-bisphosphate; F-1-P, fructorse-1-phospahte; FruK,

fructose-1-phospahte Kinase; LacI, lactose repressor protein; LLhF, LacI-Cra chimera.

References

1. Ramseier, T. M. (1996) Cra and the control of carbon flux via metabolic pathways. *Res. Microbiol.* **147**, 489–493
2. Saier, M. H., Jr., and Ramseier, T. M. (1996) The catabolite repressor/activator (Cra) protein of enteric bacteria. *J. Bacteriol.* **178**, 3411–3417
3. Saier, M. H., Jr. (1996) Cyclic AMP-independent catabolite repression in bacteria. *FEMS Microbiol. Lett.* **138**, 97–103
4. Shimada, T., Fujita, N., Maeda, M., and Ishihama, A. (2005) Systematic search for the Cra-binding promoters using genomic SELEX system. *Genes Cells* **10**, 907–918
5. Shimada, T., Yamamoto, K., and Ishihama, A. (2011) Novel members of the Cra regulon involved in carbon metabolism in Escherichia coli. *J. Bacteriol.* **193**, 649–659
6. Kim, D., Seo, S. W., Gao, Y., Nam, H., Guzman, G. I., Cho, B. K., *et al.* (2018) Systems assessment of transcriptional regulation on central carbon metabolism by Cra and CRP. *Nucleic Acids Res.* **46**, 2901–2917
7. Ramseier, T. M., Negre, D., Cortay, J. C., Scarabel, M., Cozzone, A. J., and Saier, M. H., Jr. (1993) In vitro binding of the pleiotropic transcriptional regulatory protein, FruR, to the fru, pps, ace, pts and icd operons of Escherichia coli and Salmonella typhimurium. *J. Mol. Biol.* **234**, 28–44
8. Ravcheev, D. A., Khoroshkin, M. S., Laikova, O. N., Tsoy, O. V., Sernova, N. V., Petrova, S. A., *et al.* (2014) Comparative genomics and evolution of regulons of the LacI-family transcription factors. *Front Microbiol.* **5**, 294
9. Shimizu, K. (2013) Metabolic regulation of a bacterial cell system with Emphasis on Escherichia coli metabolism ISRN. *Biochem* **2013**, 645983
10. Kornberg, H. L. (2001) Routes for fructose utilization by Escherichia coli. *J. Mol. Microbiol. Biotechnol.* **3**, 355–359
11. Ferenci, T., and Kornberg, H. L. (1973) The utilization of fructose by Escherichia coli. Properties of a mutant defective in fructose 1-phosphate kinase activity. *Biochem. J.* **132**, 341–347
12. Reizer, J., Reizer, A., Kornberg, H. L., and Saier, M. H., Jr. (1994) Sequence of the fruB gene of Escherichia coli encoding the diphosphoryl transfer protein (DTP) of the phosphoenolpyruvate: sugar phosphotransferase system. *FEMS Microbiol. Lett.* **118**, 159–162
13. Curtis, M. M., Hu, Z., Klimko, C., Narayanan, S., Deberardinis, R., and Sperandio, V. (2014) The gut commensal Bacteroides thetaiotaomicron exacerbates enteric infection through modification of the metabolic landscape. *Cell Host Microbe* **16**, 759–769
14. Zhu, Y., Gao, H., Zhang, J., Zhao, J., Qi, Q., and Wang, Q. (2023) De novo design of the global transcriptional factor Cra-regulated promoters enables highly sensitive glycolysis flux biosensor for dynamic metabolic control. *Microb. Biotechnol.* **16**, 605–617
15. Kochanowski, K., Gerosa, L., Brunner, S. F., Christodoulou, D., Nikolaev, Y. V., and Sauer, U. (2017) Few regulatory metabolites coordinate expression of central metabolic genes in Escherichia coli. *Mol. Syst. Biol.* **13**, 903
16. Kochanowski, K., Volkmer, B., Gerosa, L., Haverkorn van Rijsewijk, B. R., Schmidt, A., and Heinemann, M. (2013) Functioning of a metabolic flux sensor in Escherichia coli. *Proc. Natl. Acad. Sci. U. S. A.* **110**, 1130–1135
17. Matsuoka, Y., and Shimizu, K. (2013) Catabolite regulation analysis of Escherichia coli for acetate overflow mechanism and co-consumption of multiple sugars based on systems biology approach using computer simulation. *J. Biotechnol.* **168**, 155–173
18. Chavarria, M., Santiago, C., Platero, R., Krell, T., Casasnovas, J. M., and de Lorenzo, V. (2011) Fructose 1-phosphate is the preferred effector of the metabolic regulator Cra of Pseudomonas putida. *J. Biol. Chem.* **286**, 9351–9359
19. Chavarria, M., Durante-Rodriguez, G., Krell, T., Santiago, C., Brezovsky, J., Damborsky, J., *et al.* (2014) Fructose 1-phosphate is the one and only physiological effector of the Cra (FruR) regulator of Pseudomonas putida. *FEBS Open Bio* **4**, 377–386
20. Bley Folly, B., Ortega, A. D., Hubmann, G., Bonsing-Vedelaar, S., Wijma, H. J., van der Meulen, P., *et al.* (2018) Assessment of the interaction between the flux-signaling metabolite fructose-1,6-bisphosphate and the bacterial transcription factors CggR and Cra. *Mol. Microbiol.* **109**, 278–290
21. Usuda, Y., Nishio, Y., Iwatani, S., Van Dien, S. J., Imaizumi, A., Shimbo, K., *et al.* (2010) Dynamic modeling of Escherichia coli metabolic and regulatory systems for amino-acid production. *J. Biotechnol.* **147**, 17–30
22. Orchard, L. M., and Kornberg, H. L. (1990) Sequence similarities between the gene specifying 1-phosphofructokinase (fruK), genes specifying other kinases in Escherichia coli K12, and lacC of Staphylococcus aureus. *Proc. Biol. Sci.* **242**, 87–90
23. Veiga-da-Cunha, M., Hoyoux, A., and Van Schaftingen, E. (2000) Overexpression and purification of fructose-1-phosphate kinase from Escherichia coli: application to the assay of fructose 1-phosphate. *Protein Expr. Purif.* **19**, 48–52
24. Weeramange, C. J., Fairlamb, M. S., Singh, D., Fenton, A. W., and Swint-Kruse, L. (2020) The strengths and limitations of using biolayer interferometry to monitor equilibrium titrations of biomolecules. *Protein Sci.* **29**, 1018–1034
25. Meinhardt, S., Manley, M. W., Jr., Becker, N. A., Hessman, J. A., Maher, L. J., 3rd, and Swint-Kruse, L. (2012) Novel insights from hybrid LacI/GalR proteins: family-wide functional attributes and biologically significant variation in transcription repression. *Nucleic Acids Res.* **40**, 11139–11154
26. Bennett, B. D., Kimball, E. H., Gao, M., Osterhout, R., Van Dien, S. J., and Rabinowitz, J. D. (2009) Absolute metabolite concentrations and implied enzyme active site occupancy in Escherichia coli. *Nat. Chem. Biol.* **5**, 593–599
27. Mancini, F., Fiori, J., Cavrini, V., and Andrisano, V. (2006) Separation and quantitation of fructose-6-phosphate and fructose-1 ,6-diphosphate by LC-ESI-MS for the evaluation of fructose-1,6-biphosphatase activity. *J. Sep. Sci.* **29**, 2395–2400
28. Buescher, J. M., Moco, S., Sauer, U., and Zamboni, N. (2010) Ultrahigh performance liquid chromatography-tandem mass spectrometry method for fast and robust quantification of anionic and aromatic. *Metabolites Anal Chem.* **82**, 4403–4412
29. Tungtur, S., Skinner, H., Zhan, H., Swint-Kruse, L., and Beckett, D. (2011) In vivo tests of thermodynamic models of transcription repressor function. *Biophysical Chem.* **159**, 142–151
30. Gilbert, W., and Maxam, A. (1973) The nucleotide sequence of the lac operator. *Proc. Natl. Acad. Sci. U. S. A.* **70**, 3581–3584
31. Bledig, S. A., Ramseier, T. M., and Saier, M. H., Jr. (1996) Frur mediates catabolite activation of pyruvate kinase (pykF) gene expression in Escherichia coli. *J. Bacteriol.* **178**, 280–283
32. Sigrell, J. A., Cameron, A. D., Jones, T. A., and Mowbray, S. L. (1998) Structure of Escherichia coli ribokinase in complex with ribose and dinucleotide determined to 1.8 A resolution: insights into a new family of kinase structures. *Structure* **6**, 183–193
33. Cortay, J. C., Negre, D., Scarabel, M., Ramseier, T. M., Vartak, N. B., Reizer, J., *et al.* (1994) In vitro asymmetric binding of the pleiotropic regulatory protein, FruR, to the ace operator controlling glyoxylate shunt enzyme synthesis. *J. Biol. Chem.* **269**, 14885–14891
34. [dataset] Chang, C., Evdokimova, E., Kagan, O., Savchenko, A., Edwards, A. M., and Joachimiak, A. (2006) Midwest Center for Structural Genomics (MCSG), crystal structure of N-terminal truncated DNA-binding transcriptional dual regulator from Escherichia coli K12. *Protein Data Bank*, 2IKS
35. Swint-Kruse, L., and Matthews, K. S. (2009) Allostery in the LacI/GalR family: variations on a theme. *Curr. Opin. Microbiol.* **12**, 129–137
36. Xu, S., and Arnsdorf, M. F. (1994) Calibration of the scanning (atomic) force microscope with gold particles. *J. Microsc.* **173**, 199–210
37. Beckwitt, E. C., Kong, M., and Van Houten, B. (2018) Studying protein-DNA interactions using atomic force microscopy. *Semin. Cell Dev Biol.* **73**, 220–230
38. Fuentes-Perez, M. E., Dillingham, M. S., and Moreno-Herrero, F. (2013) AFM volumetric methods for the characterization of proteins and nucleic acids. *Methods* **60**, 113–121
39. Bell, C. E., and Lewis, M. (2000) A closer view of the conformation of the Lac repressor bound to operator. *Nat. Struct. Biol.* **7**, 209–214

ASBMB

40. Glasfeld, A., Koehler, A. N., Schumacher, M. A., and Brennan, R. G. (1999) The role of lysine 55 in determining the specificity of the purine repressor for its operators through minor groove interactions. *J. Mol. Biol.* **291**, 347–361
41. Bond, L. M., Peters, J. P., Becker, N. A., Kahn, J. D., and Maher, L. J., 3rd (2010) Gene repression by minimal lac loops in vivo. *Nucleic Acids Res.* **38**, 8072–8082
42. Becker, N. A., Kahn, J. D., and Maher, L. J., 3rd (2005) Bacterial repression loops require enhanced DNA flexibility. *J. Mol. Biol.* **349**, 716–730
43. Lia, G., Bensimon, D., Croquette, V., Allemand, J. F., Dunlap, D., Lewis, D. E., *et al.* (2003) Supercoiling and denaturation in Gal repressor/heat unstable nucleoid protein (HU)-mediated DNA looping. *Proc. Natl. Acad. Sci. U. S. A.* **100**, 11373–11377
44. Eismann, E. R., and Muller-Hill, B. (1990) Lac repressor forms stable loops in vitro with supercoiled wild-type lac DNA containing all three natural lac operators. *J. Mol. Biol.* **213**, 763–775
45. Whitson, P. A., Hsieh, W. T., Wells, R. D., and Matthews, K. S. (1987) Supercoiling facilitates lac operator-repressor-pseudooperator interactions. *J. Biol. Chem.* **262**, 4943–4946
46. Mossing, M. C., and Record, M. T., Jr. (1986) Upstream operators enhance repression of the lac promoter. *Science* **233**, 889–892
47. Matthews, K. S. (1992) DNA looping. *Microbiol. Rev.* **56**, 123–136
48. Oehler, S., Eismann, E. R., Kramer, H., and Muller-Hill, B. (1990) The three operators of the lac operon cooperate in repression. *EMBO J.* **9**, 973–979
49. Molchanova, M. L., Erdagaeva, R. S., Grigorenko Iu, A., Bol'shakova, T. N., and Gershanovich, V. N. (1992) Role of fructose-1-phosphate kinase in expression of PEP-synthase in Escherichia coli K-12 *Genetika* **28**, 46–51
50. Chin, A. M., Feldheim, D. A., and Saier, M. H., Jr. (1989) Altered transcriptional patterns affecting several metabolic pathways in strains of Salmonella typhimurium which overexpress the fructose regulon. *J. Bacteriol.* **171**, 2424–2434
51. Baba, T., Ara, T., Hasegawa, M., Takai, Y., Okumura, Y., Baba, M., *et al.* (2006) Construction of Escherichia coli K-12 in-frame, single-gene knockout mutants: the Keio collection. *Mol. Syst. Biol.* **2**, 2006.0008
52. Reshamwala, S. M., and Noronha, S. B. (2011) Biofilm formation in Escherichia coli cra mutants is impaired due to down-regulation of curli biosynthesis. *Arch. Microbiol.* **193**, 711–722
53. Ishihama, A., Shimada, T., and Yamazaki, Y. (2016) Transcription profile of Escherichia coli: genomic SELEX search for regulatory targets of transcription factors. *Nucleic Acids Res.* **44**, 2058–2074
54. Vemulapalli, S., Hashemi, M., Kolomeisky, A. B., and Lyubchenko, Y. L. (2021) DNA looping mediated by site-specific SfiI-DNA interactions. *J. Phys. Chem. B* **125**, 4645–4653
55. Peters, J. P., 3rd, and Maher, L. J. (2010) DNA curvature and flexibility in vitro and in vivo. *Q. Rev. Biophys.* **43**, 23–63
56. Njoroge, J. W., Nguyen, Y., Curtis, M. M., Moreira, C. G., and Sperandio, V. (2012) Virulence meets metabolism: cra and KdpE gene regulation in enterohemorrhagic Escherichia coli. *mBio* **3**
57. Ramseier, T. M., Chien, S. Y., and Saier, M. H., Jr. (1996) Cooperative interaction between Cra and Fnr in the regulation of the cydAB operon of Escherichia coli. *Curr. Microbiol.* **33**, 270–274
58. Bhende, P. M., and Egan, S. M. (2000) Genetic evidence that transcription activation by RhaS involves specific amino acid contacts with sigma 70. *J. Bacteriol.* **182**, 4959–4969
59. Dhiman, A., and Schleif, R. (2000) Recognition of overlapping nucleotides by AraC and the sigma subunit of RNA polymerase. *J. Bacteriol.* **182**, 5076–5081
60. Wickstrum, J. R., and Egan, S. M. (2004) Amino acid contacts between sigma 70 domain 4 and the transcription activators RhaS and RhaR. *J. Bacteriol.* **186**, 6277–6285
61. Swint-Kruse, L., Zhan, H., and Matthews, K. S. (2005) Integrated insights from simulation, experiment, and mutational analysis yield new details of LacI function. *Biochemistry* **44**, 11201–11213
62. Jones, D. H. (1994) PCR mutagenesis and recombination in vivo. *PCR Methods Appl.* **3**, S141–S148
63. Qaidi, S. E., and Hardwidge, P. R. (2019) ABC cloning: an efficient, simple, and rapid restriction/ligase-free method. *MethodsX* **6**, 316–321
64. Altschul, S. F., Madden, T. L., Schaffer, A. A., Zhang, J., Zhang, Z., Miller, W., *et al.* (1997) Gapped BLAST and PSI-BLAST: a new generation of protein database search programs. *Nucleic Acids Res.* **25**, 3389–3402
65. Larkin, M. A., Blackshields, G., Brown, N. P., Chenna, R., McGettigan, P. A., McWilliam, H., *et al.* (2007) Clustal W and clustal X version 2.0. *Bioinformatics* **23**, 2947–2948
66. Ashkenazy, H., Abadi, S., Martz, E., Chay, O., Mayrose, I., Pupko, T., *et al.* (2016) ConSurf 2016: an improved methodology to estimate and visualize evolutionary conservation in macromolecules. *Nucleic Acids Res.* **44**, W344–W350
67. Falcon, C. M., and Matthews, K. S. (2001) Engineered disulfide linking the hinge regions within lactose repressor dimer increases operator affinity, decreases sequence selectivity, and alters allostery. *Biochemistry* **40**, 15650–15659
68. Swint-Kruse, L., Zhan, H., Fairbanks, B. M., Maheshwari, A., and Matthews, K. S. (2003) Perturbation from a distance: mutations that alter LacI function through long-range effects. *Biochemistry* **42**, 14004–14016
69. Taraban, M., Zhan, H., Whitten, A. E., Langley, D. B., Matthews, K. S., Swint-Kruse, L., *et al.* (2008) Ligand-induced conformational changes and conformational dynamics in the solution structure of the lactose repressor protein. *J. Mol. Biol.* **376**, 466–481
70. Zhan, H., Swint-Kruse, L., and Matthews, K. S. (2006) Extrinsic interactions dominate helical propensity in coupled binding and folding of the lactose repressor protein hinge helix. *Biochemistry* **45**, 5896–5906
71. Wycuff, D. R., and Matthews, K. S. (2000) Generation of an Ara-C-*ara*-BAD promoter-regulated T7 expression system. *Anal. Biochem.* **277**, 67–73
72. Chen, J., and Matthews, K. S. (1992) T41 mutation in lac repressor is Tyr282——Asp. *Gene* **111**, 145–146
73. [preprint] Singh, D., Fairlamb, M. S., Harrison, K. S., Weeramange, C., Meinhardt, S., Tungtur, S., *et al.* (2017) Protein-protein interactions with fructose-1-kinase alter function of the central *Escherichia coli* transcription regulator, Cra. *bioRxiv*. https://doi.org/10.1101/201277
74. Swint-Kruse, L., and Matthews, K. S. (2004) Thermodynamics, protein modification, and molecular dynamics in characterizing lactose repressor protein: strategies for complex analyses of protein structure-function. *Methods Enzymol.* **379**, 188–209
75. Neidhardt, F. C., Bloch, P. L., and Smith, D. F. (1974) Culture medium for enterobacteria. *J. Bacteriol.* **119**, 736–747
76. Bhende, P. M., and Egan, S. M. (1999) Amino acid-DNA contacts by RhaS: an AraC family transcription activator. *J. Bacteriol.* **181**, 5185–5192
77. Meinhardt, S., and Swint-Kruse, L. (2008) Experimental identification of specificity determinants in the domain linker of a LacI/GalR protein: bioinformatics-based predictions generate true positives and false negatives. *Proteins* **73**, 941–957
78. Laemmli, U. K. (1970) Cleavage of structural proteins during the assembly of the head of bacteriophage T4. *Nature* **227**, 680–685
79. *Molecular Devices, Octet® and BLItz® Systems: Thickness Display in the Y-axis Molecular Devices.* (2019). ForteBio, Menol Park, CA
80. Concepcion, J., Witte, K., Wartchow, C., Choo, S., Yao, D., Persson, H., *et al.* (2009) Label-free detection of biomolecular interactions using BioLayer interferometry for kinetic characterization. *Comb. Chem. High Throughput Screen.* **12**, 791–800
81. Riley-Lovingshimer, M. R., and Reinhart, G. D. (2005) Examination of MgATP binding in a tryptophan-shift mutant of phosphofructokinase from Bacillus stearothermophilus. *Arch. Biochem. Biophys.* **436**, 178–186
82. Lyubchenko, Y. L., and Shlyakhtenko, L. S. (2009) AFM for analysis of structure and dynamics of DNA and protein-DNA complexes. *Methods* **47**, 206–213
83. Hermanowicz, P., Sarna, M., Burda, K., and Gabrys, H. (2014) AtomicJ: an open source software for analysis of force curves. *Rev. Sci. Instrum.* **85**, 063703
84. Sigrell, J. A., Cameron, A. D., and Mowbray, S. L. (1999) Induced fit on sugar binding activates ribokinase. *J. Mol. Biol.* **290**, 1009–1018

85. Pettersen, E. F., Goddard, T. D., Huang, C. C., Couch, G. S., Greenblatt, D. M., Meng, E. C., *et al.* (2004) UCSF Chimera–a visualization system for exploratory research and analysis. *J. Comput. Chem.* **25**, 1605–1612
86. Okuyama, M., Mori, H., Chiba, S., and Kimura, A. (2004) Overexpression and characterization of two unknown proteins, Yici Yihq, originated Escherichia coli. *Protein Expr. Purif.* **37**, 170–179
87. Carneiro, L., Fuzo, C. A., Meleiro, L. P., Carli, S., Barreto, M. Q., Lourenzoni, M. R., *et al.* (2022) Selective xyloglucan oligosaccharide hydrolysis by a GH31 α-xylosidase from Escherichia coli. *Carbohydr. Polym.* **284**, 119150
88. Répérant, M., Porcheron, G., Rouquet, G., and Gilot, P. (2011) The yicJI metabolic operon of Escherichia coli is involved in bacterial fitness. *FEMS Microbiol. Lett.* **319**, 180–186
89. Hall, B. G., Acar, H., Nandipati, A., and Barlow, M. (2014) Growth rates made easy. *Mol. Biol. Evol.* **31**, 232–238
90. Meinhardt, S., Manley, M. W., Jr., Parente, D. J., and Swint-Kruse, L. (2013) Rheostats and toggle switches for modulating protein function. *PLoS One* **8**, e83502
91. Swint-Kruse, L., Martin, T. A., Page, B. M., Wu, T., Gerhart, P. M., Dougherty, L. L., *et al.* (2021) Rheostat functional outcomes occur when substitutions are introduced at nonconserved positions that diverge with speciation. *Protein Sci.* **30**, 1833–1853
92. Bachmann, B. J. (1972) Pedigrees of some mutant strains of Escherichia-coli K-12. *Bacteriol. Rev.* **36**, 525–557
93. Stewart, G. S., Lubinsky-Mink, S., Jackson, C. G., Cassel, A., and Kuhn, J. (1986) pHG165: a pBR322 copy number derivative of pUC8 for cloning and expression. *Plasmid* **15**, 172–181
94. Perna, N. T., Plunkett, G., 3rd, Burland, V., Mau, B., Glasner, J. D., Rose, D. J., *et al.* (2001) Genome sequence of enterohaemorrhagic Escherichia coli O157:H7. *Nature* **409**, 529–533
95. Neetu, N., Katiki, M., Mahto, J. K., Sharma, M., Narayanan, A., Maity, S., *et al.* (2021) Deciphering the enigma of missing DNA binding domain of LacI family transcription factors. *Arch. Biochem. Biophys.* **713**, 109060
96. Geisler, N., and Weber, K. (1978) Escherichia coli lactose repressor: isolation of two different homogeneous headpieces and the existence of a hinge region between residues 50 and 60 in the repressor molecule. *FEBS Lett.* **87**, 215–218
97. Geisler, N., and Weber, K. (1977) Isolation of amino-terminal fragment of lactose repressor necessary for DNA binding. *Biochemistry* **16**, 938–943
98. Files, J. G., and Weber, K. (1976) Limited proteolytic digestion of lac repressor by trypsin. Chem. Nat. resulting trypsin-resistant core. *J Biol. Chem.* **251**, 3386–3391